

Enhancing Descriptive Image Quality Assessment with A Large-scale Multi-modal Dataset

Zhiyuan You, Jinjin Gu, Xin Cai, Zheyuan Li, Kaiwen Zhu, Chao Dong[†], Tianfan Xue[†]

Abstract—With the rapid advancement of Vision Language Models (VLMs), VLM-based Image Quality Assessment (IQA) seeks to describe image quality linguistically to align with human expression and capture the multifaceted nature of IQA tasks. However, current methods are still far from practical usage. First, prior works focus narrowly on specific sub-tasks or settings, which do not align with diverse real-world applications. Second, their performance is sub-optimal due to limitations in dataset coverage, scale, and quality. To overcome these challenges, we introduce the enhanced *Depicted* image Quality Assessment model (DepictQA-Wild). Our method includes a multi-functional IQA task paradigm that encompasses both assessment and comparison tasks, brief and detailed responses, full-reference and non-reference scenarios. We introduce a ground-truth-informed dataset construction approach to enhance data quality, and scale up the dataset to 495K under the brief-detail joint framework. Consequently, we construct a comprehensive, large-scale, and high-quality dataset, named DQ-495K. We also retain image resolution during training to better handle resolution-related quality issues, and estimate a confidence score that is helpful to filter out low-quality responses. Experimental results demonstrate that DepictQA-Wild significantly outperforms traditional score-based methods, prior VLM-based IQA models, and proprietary GPT-4V in distortion identification, instant rating, and reasoning tasks. Our advantages are further confirmed by real-world applications including assessing the web-downloaded images and ranking model-processed images. Codes, datasets, and model weights have been released in <https://depictqa.github.io/>.

I. INTRODUCTION

IMAGE Quality Assessment (IQA) aims to measure and compare the quality of images, expecting to align with human perception. With the emergence of Vision Language

Models (VLMs) [1]–[3], VLM-based IQA begins to attract more research interest [4]–[8]. These methods leverage VLMs to describe image quality using language, recognizing that language better mirrors human expression, and captures the multifaceted nature of IQA tasks [8]. However, existing VLM-based IQA methods still fall short especially in aspects of *functionality* and *performance*.

Functionality. There are various application scenarios of IQA, but existing VLM-based IQA models only support a few of them. For example, one scenario involves assessing a single image downloaded from the web, while another requires comparing multiple images handled by different algorithms. Also, image restoration needs to assess an image against a reference, while image generation requests non-reference assessments. Therefore, a superior IQA model should be multi-functional to cater to such diverse scenarios. However, existing methods limit to a specific subset of these tasks, such as single-image assessment [5], multi-image comparison [6], or full-reference setting [8], *etc.* Hence, the limitations in functionality hinder the wide applications of prior methods.

Performance. Many IQA methods perform well on some specific datasets but may generalize poorly to other images with different contents or distortions. For instance, Co-Instruct [6] performs well on TID2013 dataset [9] (85.0%), but drops significantly to 50.7% when testing on BAPPS dataset [10]. A more comprehensive comparison on our newly created benchmark is given in Fig. 1, where it shows that previous works [5], [6] under-perform even within their defined tasks and settings. One potential cause for this is the limited scope of their training datasets. For example, the added distortion category in Q-Instruct [5] is limited; Co-Instruct [6] directly utilizes GPT-4V [2], which is not accurate in IQA tasks, to generate data; and the dataset scale in DepictQA [8] remains small. Besides, these methods are constrained in their usage by resizing images to a fixed resolution [5], [6], while the image resolution is critical for quality. Therefore, the dataset’s coverage, quality, and scale together with the training techniques limit the performance of previous methods.

To address these challenges, we propose a multi-functional IQA model to handle various image quality assessment tasks. We categorize these tasks into two types, as shown in Fig. 2. (a) *Single-image assessment* aims to evaluate the quality of a single image by identifying distortions (*e.g.*, “blur” in Fig. 2a top). It can also analyze the distortions’ impacts on contents (*e.g.*, blur “affecting the definition of mountains and trees” in Fig. 2a bottom). (b) *Paired-image comparison* focuses on comparing the quality of two distorted images based on the clarity, colorfulness, and sharpness of presented contents.

Corresponding author: Tianfan Xue, Chao Dong. This work was sponsored by RGC Early Career Scheme (ECS) No. 24209224, National Natural Science Foundation of China (Grant No.62276251), and the Joint Lab of CAS-HK.

Zhiyuan You is with Multimedia Laboratory, The Chinese University of Hong Kong, Hong Kong 999077, China, and also with Shenzhen Institutes of Advanced Technology, Chinese Academy of Sciences, Shenzhen 518055, China. (e-mail: zhiyuanyou@link.cuhk.edu.hk)

Jinjin Gu is with INSAIT, Sofia University, Sofia 1784, Bulgaria. (e-mail: jinjin.gu@insait.ai)

Xin Cai is with Multimedia Laboratory, The Chinese University of Hong Kong, Hong Kong 999077, China. (e-mail: caixin@link.cuhk.edu.hk)

Zheyuan Li is with University of Macau, Macau 999078, China, and also with Shenzhen Institutes of Advanced Technology, Chinese Academy of Sciences, Shenzhen 518055, China. (e-mail: zheyuanli884886@gmail.com)

Kaiwen Zhu is with Shanghai Jiao Tong University, Shanghai 200240, China, and also with Shanghai Artificial Intelligence Laboratory, Shanghai 200232, China. (e-mail: sqzhukaiwen@sjtu.edu.cn)

Chao Dong is with Shenzhen Institutes of Advanced Technology, Chinese Academy of Sciences, and also with Shenzhen University of Advanced Technology, Shenzhen 518055, China. (e-mail: chao.dong@siat.ac.cn)

Tianfan Xue is with Multimedia Laboratory, The Chinese University of Hong Kong, Hong Kong 999077, China, CPIX under InnoHK, Hong Kong 999077, China, and also with Shanghai Artificial Intelligence Laboratory, Shanghai 200232, China. (e-mail: txfue@ie.cuhk.edu.hk)

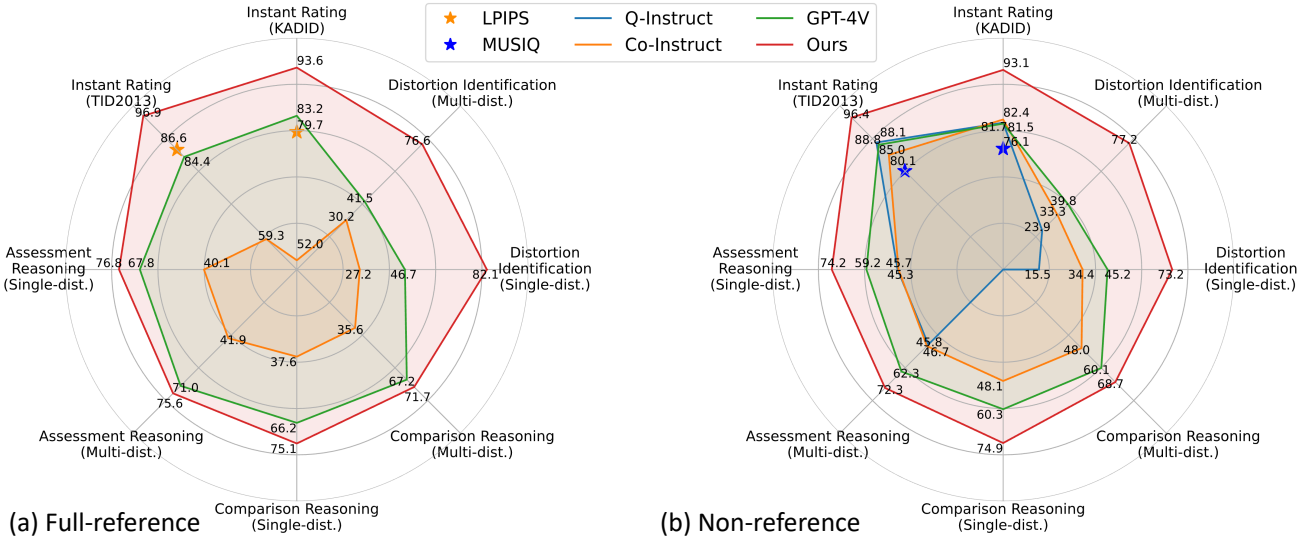


Fig. 1: **Performance comparison.** Our model surpasses previous works including Q-Instruct [5], Co-Instruct [6], and the proprietary GPT-4V [2] across a broad range of tasks in both full-reference and non-reference settings. Traditional score-based IQA methods like LPIPS [10] and MUSIQ [11] have no language abilities, and thus can only be used in *instant rating* task. Q-Instruct is only tested on single-image input tasks.

For example, in Fig. 2b, despite reduced contrast, “Image A maintains more scene integrity”, as “Image B’s serious noise level is more detrimental”. We omit multi-image comparison since it is an easy extension of a pairwise one [12]. Each type includes basic *brief* sub-tasks for fundamental assessments and *detailed* sub-tasks to enhance reasoning abilities. Moreover, the model supports both *full-reference* and non-reference settings, making it adaptable to diverse scenarios.

Under the multi-functional task paradigm, we construct a new large-scale dataset, DQ-495K, for comprehensive and accurate training and evaluation. First, for diverse distortion, we design and implement 35 types of distortions, each with 5 levels. Second, to enhance the label quality, we inform GPT-4V of the low-level ground truths (e.g., distortions) to leverage its strong high-level perception and language abilities, while avoiding its sub-optimal IQA capabilities. Third, to increase the dataset scale, we scale up the data amount to 495K under the brief-detail combined framework [8]. Also, our dataset is suitable for both full-reference and non-reference settings.

With the above collected DQ-495K dataset, we then train an enhanced **Depicted image Quality Assessment VLM** model (DepictQA-Wild). During training, the original image resolution is retained, leading to a better quality perception regarding resolution. Furthermore, we estimate the confidence of responses from key tokens, providing vital auxiliary information, especially for filtering low-quality responses.

The performance of DepictQA-Wild is evaluated in Fig. 1 and Sec. V. In brief tasks, our model surpasses general VLMs, IQA-specific VLMs, and score-based IQA methods by a large margin. For example, we achieve 95.9% in non-reference comparison on TID2013 dataset, remarkably surpassing Co-Instruct (85.0%) and GPT-4V (88.1%). In detailed tasks, our model also excels, e.g., recording 74.9% in non-reference comparison reasoning, compared to 48.1% for Co-Instruct and 60.3% for GPT-4V. At last, experiments on real-world applications including assessing web-downloaded images and

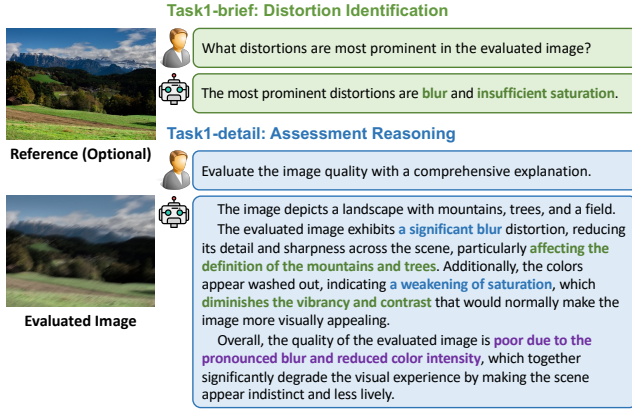
comparing model-restored images further demonstrate our superiority. We hope that our multi-functional model could serve as a stepping stone towards a unified VLM-based IQA model. Although not yet fully realized, our method showcases the potential of VLM-based IQA models.

II. RELATED WORKS

Score-based IQA methods. Traditional IQA methods rely on scores to assess image quality and can be divided into *full-reference* and *non-reference* methods. (a) Full-reference methods compute a similarity score between a distorted image and a high-quality reference. Early works rely on human-designed metrics such as image information [13], structural similarity [14], phase congruency with gradient magnitude [15], *etc.* The rapid advancement of deep learning has also inspired learning-based IQA methods that measure image quality through data-driven training. Pioneered by PieAPP [16] and LPIPS [10], data-driven approaches [17]–[23] have spurred innovations in IQA, exhibiting high consistency with human judgments. (b) Non-reference methods directly regress a quality score without a reference image. Initially, human-designed natural image statistics are adopted [24]–[30]. Subsequently, deep-learning-based methods [31]–[37] replace hand-crafted statistics by learning quality priors from extensive data. Recent works focus on enhancing performance by introducing multi-scale features [11], CLIP pre-training [38], multi-dimension attention [39], continual learning [40], multitask learning [41], and so on. However, as discussed in [8], score-based IQA methods limit themselves in complex analyses and multi-aspect weighing of IQA, since the information provided by a single score is far from sufficient.

Vision Language Models (VLMs) incorporate visual modality into Large Language Models (LLMs) [42]–[44], aiming to leverage their emergent ability to achieve general visual ability. These VLMs [1], [2], [45]–[52] have demonstrated

(a) Task1: Single-image Assessment



(b) Task2: Paired-image Comparison

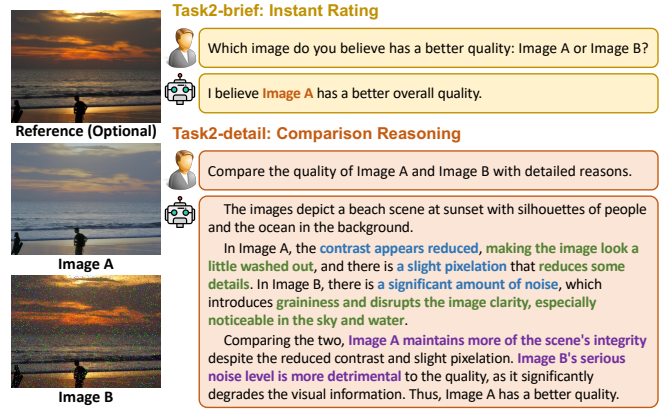


Fig. 2: **Illustration of our task paradigm and qualitative results.** Our DepictQA-Wild focuses on two main tasks including *single-image assessment* and *paired-image comparison* in both *full-reference* and *non-reference* settings. Each task contains a *brief* sub-task focusing on the fundamental IQA ability, and a *detailed* sub-task fostering the reasoning capacities. More qualitative results are provided in Fig. S5 and S7 of *Supp. Mat.*

a general visual ability and can tackle a variety of multi-modality tasks, including image captioning [53]–[55], visual question answering [56]–[58], document understanding [59]–[61], *etc.* Although proficient in these high-level visual perception tasks, we demonstrate in Sec. V that general-purpose VLMs still struggle with IQA tasks.

VLM-based IQA methods aim to achieve better alignment with human perception leveraging the power of VLMs [7]. Q-Bench [4] establishes a comprehensive benchmark for evaluating general-purpose VLMs in low-level perception tasks. [62] evaluates various VLMs on the widely-adopted two-alternative forced choice (2AFC) task. Q-Instruct [5] enhances the low-level perception ability of VLMs by introducing a large-scale dataset. Q-Align [63] and DeQA-Score [64] employ discrete text-defined levels for more accurate quality score regression. Co-Instruct [6] concentrates on the quality comparison among multiple images. DepictQA [8] performs quality description, quality comparison, and comparison reasoning in the full-reference setting. Recently, inspired by the success of DeepSeek-R1 [65], Q-Insight [66] first introduces reasoning-induced quality regression by employing the GRPO reinforcement learning method [67] for IQA. Building upon this idea, VisualQuality-R1 [68] further improves IQA performance by incorporating pairwise ranking relationships into the reinforcement learning objective. Moreover, Q-Ponder [69] proposes a unified two-stage training framework, consisting of a cold-start pretraining phase followed by reinforcement learning-based fine-tuning. Nonetheless, as highlighted in Sec. I, most of these methods focus on specific aspects of IQA tasks, diverging from the original intents of VLMs’ universality and practical usage requirements.

Explainable AI for computer vision. Our descriptive IQA model could be seen as an explainable IQA approach, as it provides a human-understandable reasoning process. Recent studies in computer vision have increasingly emphasized explainability to enhance transparency and trust in deep models [70]–[74]. Several efforts have also been made to design explainable IQA models [75]–[77]. However, most existing explainable IQA methods primarily rely on visualization-based

interpretability (*i.e.*, saliency or attribution maps) to highlight influential regions, which can qualitatively indicate what the model attends to but fails to fully capture the underlying reasoning or perceptual logic behind the score assignment. Recently, TIFA [78] leveraged language-based question answering to evaluate text-to-image results, demonstrating that linguistic explanations can serve as an intuitive bridge between human judgment and model understanding. Inspired by this, we take a further step to construct a descriptive IQA model that provides natural-language rationales to describe perceptual factors influencing the assessment.

III. TASK PARADIGM AND DATASET CONSTRUCTION

A. Task Paradigm

As highlighted in the introduction, there are various application scenarios for IQA models. First, the evaluation objective can be either single-image assessment or paired-image comparison. The former is useful to rate a web-downloaded image, while the latter suits comparing images processed by two different algorithms. Second, the reference setting may be full-reference or non-reference. For example, image restoration requires assessments based on references, while image generation needs non-reference evaluations. Third, the response could be either brief or detailed. Brief responses suit well-targeted tasks (*e.g.*, comparison without reasons), while detailed responses enhance interpretability and human interaction. To cater to such diverse scenarios, a practical IQA method should be multi-functional. Therefore, we aim to establish such a multi-functional task paradigm for VLM-based IQA research. As shown in Fig. 2, we focus on two tasks, each containing both brief and detailed sub-tasks, and supporting both full-reference and non-reference settings.

- *Task1: single-image assessment.* (a) Brief sub-task: *distortion identification*. Given a distorted image, the model should identify the most obvious distortions. (b) Detailed sub-task: *assessment reasoning*. In addition to identifying distortions, the model should also describe how these

TABLE I: Overview of our distortion library with 12 super-categories and 35 sub-categories in total.

Super-category	Blur	Noise	Compression	Brighten	Darken	Contrast Strengthen	Contrast Weaken	Saturate Strengthen	Saturate Weaken	Over-sharpen	Pixelate	Quantize
# Sub-category	6	6	2	4	4	2	2	2	2	1	1	3

distortions affect the perception of image contents and the overall image quality.

- *Task2: paired-image comparison.* (a) Brief sub-task: *instant rating*. Given two distorted images, the model should find the image with better quality. (b) Detailed sub-task: *comparison reasoning*. Building upon the comparison results, the model should first compare the content loss caused by distortions in the two images, then weigh different aspects to draw inferences, and finally justify its comparison results. Note that we omit the multi-image (>2) comparison since it can be achieved easily as the extension of paired case [12].

Compared with previous works, our design unifies various tasks, response types, and reference settings into a multi-functional paradigm. In contrast, Q-Instruct [5] focuses on non-reference single-image assessment, Co-Instruct [6] targets comparison among multiple images in the non-reference setting, and DepictQA [8] primarily addresses the full-reference setting. Although one can achieve unified IQA by combining these task-specific IQA models, it is impractical due to the significant increase in network parameters, considering that current VLMs are already quite large.

B. Distortion Library

Existing IQA datasets (e.g., BAPPS [10], PieAPP [16]) usually introduce distortions (e.g., noise, blur) into high-quality reference images to create distorted images for evaluation. However, these datasets do not publicly release the distortion information of each image, and their distortions only cover limited scenes. Therefore, we aim to develop a comprehensive large-scale distortion library.

Distortion generation. Our distortion system comprises 12 super-categories in total, with each super-category consisting of multiple sub-categories. For instance, the “blur” category encompasses “Gaussian blur”, “motion blur”, “lens blur”, etc. In total, there are 35 sub-categories. For each sub-category, there are 5 severity levels: “slight”, “moderate”, “obvious”, “serious”, and “catastrophic”. A summary is illustrated in Tab. I. Considering the need to assess high-quality images as well, we retain the original image without any distortions in 5% proportion. See details in *Supp. Mat.*

Multi-distortion setups. In practical usage, multiple distortions may occur simultaneously on the same image. While a simple way to simulate them is to add multiple distortions recursively, real-world scenarios are more complex. First, one distortion may weaken another, such as “brighten” weakens “darken”, “blur” weakens “over-sharpen”. Second, certain distortions exhibit similar visual results, such as “pixelate” looks similar to “blur”, making it challenging to identify both if they are applied simultaneously. We also observe that humans can identify at most two distortions when three or more are applied, as illustrated in Fig. S2 of *Supp. Mat.* Hence, we limit the distortion number to two and manually review

all possible combinations to exclude contradictory or similar combinations. See details of multi-distortion setting in Tab. S1 and Sec. A of *Supp. Mat.*

C. Dataset Construction

High-quality and large-scale datasets are crucial for training VLMs. Following [1], [49], training VLMs requires {images, question, response} triplets, where “images” are the ones to be evaluated, “question” describes the task, and “response” is the ground truth answer. In this section, we detail the construction of our dataset from the selection of images and the collection of questions and responses.

Image collection. Typical IQA datasets involve two types of images: high-quality reference images and distorted images to be evaluated. Generating distorted images is easy given our comprehensive distortion library introduced in Sec. III-B. Existing studies often collect a large number of distorted images from a small number of references [9], [12]. However, the semantic richness of images is also crucial for VLM training. Therefore, we primarily source reference images from the KADIS-700K dataset [79], which offers 140K pristine reference images from diverse natural and daily scenes. We also leverage other IQA datasets for their convenience to generate responses (details are below).

Question collection. Humans often express similar questions using different sentences, necessitating model robustness to various questions. For each task, we initially prompt GPT-4 [43] to generate 50 candidate questions. Then, we manually eliminate ambiguous and repetitive ones and correct inaccurate ones, creating a set of 20 questions. We randomly sample these questions during training and testing to form the data pair.

Response collection. We employ two response types as shown in Fig. 3. The first comprises brief templated responses that are easy to produce, where we emphasize the *quantity* to bring robust fundamental skills. The second consists of detailed responses, where we emphasize the *quality* to enhance the advanced reasoning abilities. Existing methods to collect detailed responses mainly rely on human annotation [5], [8] and GPT-4V generation [6]. However, human annotation can be biased and vary in quality when annotators are untrained or tired [8]. Also, GPT-4V is not fully reliable since its IQA performance is still unsatisfactory as evidenced in Sec. V.

We rethink the key aspects of our desired responses and GPT-4V’s corresponding abilities, introducing *GT-informed generation* by prompting the Ground Truth (GT) details to enhance GPT-4V’s generation. Specifically, a high-quality detailed response should contain image contents, key distortions, the impacts of distortions on contents, and conclusions. While GPT-4V excels at identifying contents and analyzing impacts, it struggles with distortion identification and quality comparison, as shown in Sec. V. To compensate for that, we directly provide it with explicit GT information. The response generation for each task is detailed subsequently.

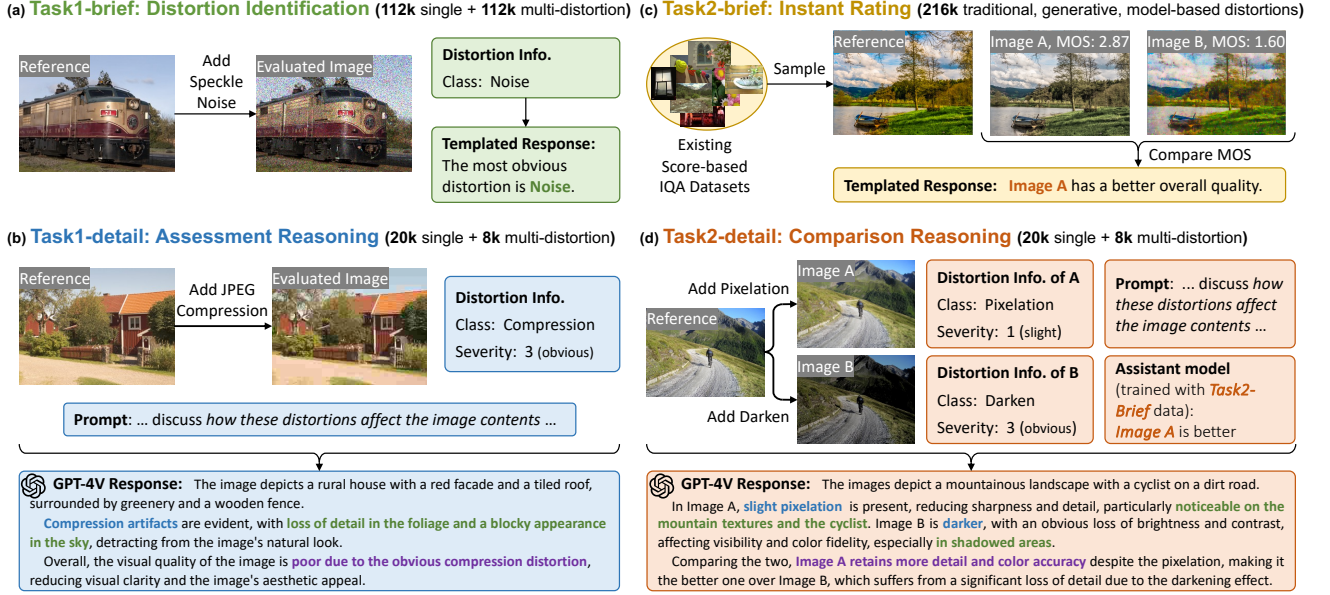


Fig. 3: **Construction of DQ-495K dataset.** For *distortion identification*, templated responses are generated using distortion information. In *instant rating*, we sample images from existing datasets and compare the Mean Opinion Score (MOS) to determine the better image for templated response creation. For *assessment reasoning* and *comparison reasoning* tasks, we provide GPT-4V with evaluated images and Ground Truth (GT) details (i.e., distortion information, comparison results from an assistant model) to facilitate detailed and accurate response generation, called *GT-informed generation*. This additional information is critical as GPT-4V cannot produce it accurately.

Task1-brief: distortion identification. As shown in Fig. 3a, we first establish a response pool containing 20 templates with unspecified distortions. Next, we add distortions into the reference to create its distorted counterpart and populate a sampled template with the specific distortions as the response. For streamlined evaluation, we sample half of the questions and append the short answer prompt: “Answer the question using a single word or phrase.” Correspondingly, the response will be a single phrase, like “noise”, specifying the distortions.

Task1-detail: assessment reasoning. Given the reference image, we initially introduce distortions to corrupt the reference. Then, GPT-4V is input with both two images and the distortion information, and requested to assess the quality of the distorted image, as illustrated in Fig. 3b. We instruct GPT-4V to respond from three dimensions: contents, distortions along with their impacts on contents, and overall quality. Prior works [5], [6] mainly focus on low-level properties, while we consider how these distortions influence the display of high-level contents.

Task2-brief: instant rating. We begin by sampling a reference image and its two distorted versions from existing IQA datasets, and then compare the Mean Opinion Score (MOS) to determine the better one, as shown in Fig. 3c. Similar to *distortion identification*, we assemble a response pool of 20 templates to convert the comparison results into textual responses, and append the short answer prompt for the convenience of evaluation. We select three IQA datasets for training, including BAPPS [10], KADID-10K [80], and PIPAL [12], to cover a diverse range of reference images.

Task2-detail: comparison reasoning. As depicted in Fig. 3d, given a high-quality image, we randomly apply distortions to produce two distorted images. We first train an assistant model using the large-scale *instant rating* data to predict the

TABLE II: **Statistics** of our DQ-495K dataset.

(a) Number of samples. All tasks except *instant rating* are displayed in the single-distortion / multi-distortion format.

	Task1-brief Distortion Identification	Task1-detail Assessment Reasoning	Task2-brief Instant Rating	Task2-detail Comparison Reasoning
Train	112,000 / 112,000	19,829 / 7,981	215,676	19,809 / 7,958
Test	28,000 / 28,000	200 / 100	41,120	200 / 100

(b) Response length reported as word count / string length.

	Distortion Identification	Assessment Reasoning	Instant Rating	Comparison Reasoning
Single-dist.	10.36 / 69.81	64.37 / 430.23		93.20 / 604.97
Multi-dist.	12.84 / 88.67	87.31 / 588.44	9.30 / 52.02	114.04 / 740.68

comparison results. Note that GPT-4V does not perform well on the quality comparison task, as shown in our experiments in Tab. IV and Tab. IX, and thus we train our own comparison model. Then, similar to *assessment reasoning*, we inform GPT-4V of the three images, distortion information, and comparison results to generate detailed responses.

Setup of non-reference setting. Our dataset accommodates both full-reference and non-reference settings. However, even for humans, identifying subtle distortions (e.g., minor brightness adjustments) without a reference is challenging. Thus, in the non-reference setting, we selectively remove samples with “slight” severity on some specific distortions, including “brighten”, “darken”, “contrast weaken”, “contrast strengthen”, “saturate weaken”, “saturate strengthen”, “quantize”, and “over-sharpen”.

D. Dataset Analysis

Dataset statistics are given in Tab. IIa. Our training set contains 439,676 brief samples and 55,577 detailed samples. For

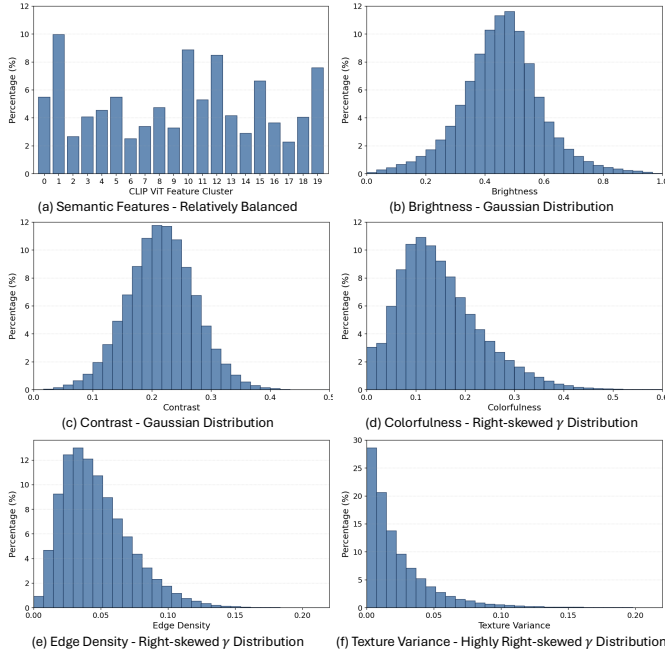


Fig. 4: **Statistics of all images** in our dataset about (a) semantic features, (b) brightness, (c) contrast, (d) colorfulness, (e) edge density, and (f) texture variance.

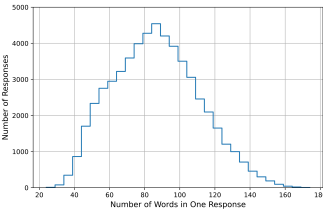


Fig. 5: **Word length distribution** of detailed responses.



Fig. 6: **Wordcloud map** of all detail responses.

instant rating, the training set includes BAPPS, KADID, and PIPAL, while the validation set consists of BAPPS, KADID, PIPAL, TID2013 [9], LIVE-MD [81], and MDID2013 [82]. To ensure there is no intersection between training and validation sets for those overlapped datasets, the original splits are kept. For detailed tasks, all samples in the validation set have been carefully checked by humans.

Image analysis. We analyze six statistical features to examine the image distributions. First, we use CLIP [83] ViT to extract semantic features and apply K-Means clustering with $k = 20$. As shown in Fig. 4a, the samples are relatively balanced across clusters. Second, the *brightness* (Fig. 4b) and *contrast* (Fig. 4c) approximately follow Gaussian distributions, consistent with natural image statistics [84]. Third, as in Fig. 4de, *colorfulness* and *edge density* exhibit right-skewed heavy-tailed distributions, which are characteristics of natural scenes [85], [86]. Finally, *texture variance* (Fig. 4f) follows a highly right-skewed γ distribution, aligning with prior findings [87]. These results confirm that our dataset maintains natural image statistics in semantic and low-level dimensions.

Text analysis. First, we examine the response length statistics of our DQ-495K dataset in Tab. IIb, including both word count and character length. For the *instant rating* task, single- and multi-distortion cases are not distinguished. We further

present the word-length distribution of detailed reasoning responses in Fig. 5. The results show a near-Gaussian distribution centered around approximately 90 words, indicating that most responses are concise yet sufficiently descriptive. Second, Fig. 6 illustrates the word cloud of our DQ-495K dataset. We manually remove “Image A” and “Image B”, as they are constant proper nouns across all texts. The most frequent terms (e.g., “overly high”, “color quantization”, “high contrast”, “high saturation”, and “detail”) are closely related to low-level image attributes and visual quality.

IV. MODEL DESIGN

Model Architecture. DepictQA-Wild primarily adopts the architecture from LLaVA-1.6 [88] and mPLUG-Owl2 [3], structured as follows. Specifically, the input images and the question texts are first tokenized, then fused, finally processed by the Large Language Model (LLM) for response generation. (1) Tokenizing input images and question texts. We use a frozen CLIP pre-trained ViT-L/14 [83] as the image encoder to convert the input images into visual tokens. The question texts are tokenized into textual tokens using the SentencePiece tokenizer [89]. To bridge the different embedding spaces of visual and textual tokens, we implement a trainable image abstractor, which is a four-layer transformer network, to map visual tokens into the textual space following [3]. The abstractor can also significantly reduce the number of vision tokens, relieving the computing pressure. (2) Token fusion. We integrate the visual tokens into pre-defined positions within the textual tokens as token fusion. (3) Response generation using LLM. The fused tokens are fed into LLM to generate the final response. Here we mainly conduct experiments with Vicuna-v1.5-7B. Despite their capabilities, pre-trained LLMs typically do not perform well on IQA tasks without adjustments. Therefore, we employ LoRA [90], a fine-tuning technique that efficiently modifies a small subset of parameters within the LLM. Specifically, we apply LoRA to adjust the projection layers in all self-attention modules, following [49], [90]. This approach allows for targeted refinement of the model’s performance on IQA tasks without the need for extensive retraining. Our experiments in Tab. XIII also show that model architecture has little influence on model performance.

Retaining resolution in training. Although previous VLM-based IQA models typically resize all input images to a fixed resolution [5], [6], we find this might hurt their performance, as resolution variation may affect visual quality. Instead, we retain the original image resolution during training. Specifically, we interpolate (in bicubic mode) the position embedding in CLIP [83] to accommodate varying image resolutions. Ablation studies detailed in Sec. V-D demonstrate our model’s capability to assess quality variations attributable to resolution, even without explicitly training on such tasks.

Confidence estimation. In many applications, it is important to know a confidence score that indicates when the model is uncertain of its response. Here we use the confidence scores of some key tokens as the confidence of the entire answer. Intuitively, the key tokens are distortion names in *distortion identification*, and are either “Image A” or “Image B” in *instant*

rating. For detailed reasoning tasks, which feature diverse and non-structured responses, we utilize semantic change testing [91] to identify the top 20 tokens with the highest importance scores as key tokens. In semantic change testing, we employ all-MiniLM-L6-v2 [92] as the similarity model, due to its high processing speed (14K sentences per second). The predicted likelihood of key tokens is averaged as the confidence score. Results in Fig. 9 verify that confidence and model performance are highly correlated.

Model setup. Since the CLIP pre-trained ViT-L/14 [83] encodes each 14×14 patch to a visual token, the resolution of the input image should be integer multiples of 14. Therefore, we first pad the size of input images to integer multiples of 14 with zero-padding. We encode the image patches into visual tokens using the CLIP pre-trained ViT-L/14 [83], with each token having a channel of 1024. The vision abstractor can reduce the number of vision tokens to 64 and map the vision tokens to the hidden dimension of the LLM, which is 4096. Without the vision abstractor, the maximum resolution is limited to 672, constrained by computation resources (RTX A6000 GPUs). However, with the vision abstractor, we can process images with much larger resolutions (up to 2500×2500). In our experiments, the maximum image resolution is 1092×1456 , thus the resolutions of all images are retained. The vision abstractor consists of four transformer layers with 64 learnable query embeddings. In LoRA of LLM, the parameters of rank and scale factor are both set as 16. The projection weights in each attention layer are fine-tuned using LoRA technique.

Training and inference setup. DepictQA-Wild is trained for 1 epoch with batch size 64. Adam optimizer with $(\beta_1, \beta_2) = (0.9, 0.95)$, weight decay 0.001, and learning rate 0.0002 is used for training. During inference, the temperature is set to 0, since lots of predicted information (e.g., distortion, comparison result) need to be certain.

V. EXPERIMENTS

A. Metrics and Baselines

Accuracy, SRCC, and PLCC. The accuracy metric is utilized for *distortion identification* and *instant rating* tasks. VLMs usually produce diverse textual outputs, and we transform them into brief results for accuracy calculation. Specifically, we prompt our model with “Answer the question using a single word or phrase” to encourage direct output of brief responses. For baseline models, we include all potential answers in the prompt and instruct the model to identify the most accurate one. We emphasize that *our key motivation is to generate descriptive language rather than quality scores*. However, our approach can produce quality scores using pairwise comparison if required. The quality scores are assessed using Spearman Rank Correlation Coefficient (SRCC) and Pearson Linear Correlation Coefficient (PLCC).

GPT-4 score, BLEU, and ROUGE-L. We employ the GPT-4 score to evaluate *assessment reasoning* and *comparison reasoning* tasks, following [1]. Specifically, we provide GPT-4 with both the model-generated response and the corresponding ground truth response. GPT-4 assesses the helpfulness, relevance, accuracy, and level of detail in the model-generated

response relative to the ground truth, assigning an overall score on a scale of 0 to 10, where a higher score indicates better quality. This average score is subsequently normalized to a scale of 0 to 100%, reported as the GPT-4 score metric. We further evaluate the reasoning tasks with classical metrics including BLEU and ROUGE-L score following [93], [94].

Baselines. We categorize our baseline methods into general-purpose VLMs and IQA-specific VLMs. For general VLMs, we include mPLUG-Owl2 [3], LLaVA-1.6 [88], LLaVA-OneVision-1.5 [95], InternVL2.5 [96], Qwen2.5-VL [97], and the proprietary GPT-4V [2]. We use 7B/8B version for open-source VLMs for fair comparison. IQA-specific VLMs are represented by Q-Instruct [5], Co-Instruct [6], CLIP-like LIQE [41], and reasoning-based IQA model Q-Insight [66]. Note that Q-Instruct only supports single-image inputs, thus we only test it on non-reference single-image assessment tasks. Additionally, we compare traditional score-based IQA methods including full-reference ones (PSNR, SSIM [14], LPIPS [10], DISTS [19]) and non-reference ones (NIQE [26], ClipIQA [38], MUSIQ [11], MANIQA [39]) in *instant rating* task and score regression experiments.

B. Results on Benchmarks

Quantitative results of distortion identification are shown in Tab. III. First, for open-source general VLMs and Co-Instruct, the performance in the non-reference setting is generally better than in the full-reference setting. This is counterintuitive, as humans typically find full-reference comparison easier. The reason is that current VLMs are primarily trained without reference, thus it is hard to use the reference image. Second, for open-source general VLMs, the performance in the multi-distortion case is higher than in the single-distortion case. In fact, for multi-distortion samples like “blur, darken”, when the model predicts only one distortion “blur”, it still achieves 0.5 accuracy. Therefore, for multi-distortion cases, achieving very high accuracy (>90%) is difficult, whereas obtaining moderate accuracy (<40%) is comparatively easier than in single-distortion cases. Third, the proprietary GPT-4V outperforms other general-purpose VLMs and exceeds specialized IQA VLMs like Q-Instruct and Co-Instruct, achieving similar results with reasoning-based IQA model Q-Insight. Fourth, DepictQA-Wild stably surpasses all baseline methods, demonstrating our model’s efficacy. Finally, we evaluate our model in an out-of-distribution (OOD) setting, i.e., for a particular category of distortion (e.g., noise), we use some sub-categories (e.g., Gaussian noise) during training, and other sub-categories (e.g., impulse noise) for evaluation. Results in the last column of Tab. III show that our method maintains high accuracy even under such an OOD setting.

Quantitative results of instant rating are demonstrated in Tab. IV. First, in the full-reference context, traditional score-based methods, even the simplest PSNR, outperform all general VLMs including GPT-4V and prior IQA-specific VLMs, indicating the inadequacy of existing VLMs in full-reference IQA tasks. Second, conversely, in the non-reference scenario, GPT-4V and Co-Instruct excel beyond most score-based approaches, except MUSIQ. Third, for some general VLMs (i.e., InternVL2.5 and Qwen2.5-VL) and IQA-specific

TABLE III: **Distortion identification results** under both single-distortion and multi-distortion cases. The accuracy metric is reported in the full-reference / non-reference settings. The best results are highlighted in **bold**. Our DepictQA-Wild greatly outperforms all baselines and maintains its high accuracy in out-of-distribution (OOD) setting.

	General VLM						IQA-specific VLM					
	mPLUG-Owl2	LLaVA-1.6	LLaVA-OV-1.5	InternVL2.5	Qwen2.5-VL	GPT-4V	Q-Instruct	Co-Instruct	LIQE	Q-Inight	Ours	Ours-OOD
Single-dist.	10.1 / 11.6	14.0 / 15.3	23.9 / 30.4	18.7 / 20.3	33.0 / 31.8	46.7 / 45.2	- / 15.5	27.2 / 34.4	- / 33.1	48.4 / 49.9	97.7 / 94.1	82.1 / 73.2
Multi-dist.	10.8 / 10.7	12.0 / 12.1	32.6 / 38.3	35.0 / 36.8	36.5 / 38.3	41.5 / 39.8	- / 23.9	30.2 / 33.3	- / 31.4	43.5 / 49.6	91.3 / 89.3	76.6 / 77.2

TABLE IV: **Instant rating results** on multiple benchmarks in the full-reference / non-reference setting with the accuracy metric. The best results are shown in **bold**. Q-Instruct is tested by inputting single images to calculate quality scores, and then compare the scores to rate. DepictQA-Wild surpasses all baselines by a large margin.

Methods		BAPPS ^{test}	KADID ^{test}	PIPAL ^{test}	TID2013	LIVE-MD	MDID2013	Mean
Full-reference Score-based IQA	PSNR	68.9 /	78.7 /	80.9 /	85.0 /	89.7 /	78.0 /	80.2 /
	SSIM	69.7 /	77.1 /	82.6 /	78.7 /	88.1 /	76.8 /	78.8 /
	LPIPS	79.4 /	79.7 /	84.2 /	86.6 /	91.3 /	85.4 /	84.4 /
	DISTS	79.7 /	85.8 /	84.6 /	87.0 /	93.1 /	88.5 /	86.5 /
Non-reference Score-based IQA	NIQE	/ 49.9	/ 66.9	/ 59.7	/ 65.0	/ 86.9	/ 82.2	/ 68.4
	ClipQA	/ 59.7	/ 75.8	/ 72.6	/ 85.8	/ 65.8	/ 47.0	/ 67.8
	MUSIQ	/ 59.2	/ 76.1	/ 77.8	/ 80.1	/ 87.2	/ 81.1	/ 76.9
	MANIQA	/ 54.9	/ 68.4	/ 79.2	/ 77.3	/ 75.4	/ 63.5	/ 69.8
General VLM	mPLUG-Owl2	50.1 / 50.1	50.6 / 50.8	49.6 / 49.6	48.6 / 48.5	49.9 / 50.1	50.6 / 50.5	49.9 / 49.9
	LLaVA-1.6	54.1 / 56.2	50.4 / 51.9	52.0 / 52.6	54.2 / 57.0	54.4 / 56.5	54.3 / 53.1	53.2 / 54.6
	LLaVA-OV-1.5	50.0 / 49.7	50.1 / 51.4	50.2 / 49.6	51.9 / 49.8	51.3 / 47.8	50.3 / 52.3	50.6 / 50.1
	InternVL2.5	50.5 / 62.8	50.2 / 75.5	50.3 / 67.0	52.4 / 83.9	52.0 / 73.0	49.4 / 73.2	50.8 / 72.6
	Qwen2.5-VL	49.6 / 55.3	55.8 / 76.2	56.7 / 67.9	61.9 / 83.3	54.5 / 64.3	50.8 / 55.6	54.9 / 67.1
	GPT-4V	70.3 / 63.2	83.2 / 81.5	78.5 / 78.2	84.4 / 88.1	79.6 / 72.7	70.6 / 67.6	77.8 / 75.2
IQA-specific VLM	Q-Instruct	- / 41.6	- / 81.7	- / 74.6	- / 88.8	- / 73.1	- / 48.5	- / 68.1
	Co-Instruct	49.8 / 50.7	52.0 / 82.4	50.6 / 72.5	59.3 / 85.0	50.0 / 70.3	50.0 / 58.0	52.0 / 69.8
	Q-Inight	49.9 / 50.8	51.1 / 85.0	63.4 / 68.6	54.2 / 90.8	48.9 / 50.7	55.8 / 58.0	53.9 / 67.3
	DepictQA-Wild	84.7 / 82.4	93.6 / 93.1	90.5 / 90.0	96.9 / 96.4	92.1 / 91.8	90.0 / 89.6	91.3 / 90.6

VLM Co-Instruct, the performance in the non-reference setting consistently surpasses that in the full-reference setting, as these models struggle to effectively utilize reference images even with explicit prompts. This further demonstrates the necessity of unifying full-reference and non-reference settings. Fourth, the reasoning-based Q-Inight model performs much better in some cases (*e.g.*, non-reference KADID and TID2013) than in others (*e.g.*, LIVE-MD and MDID2013), indicating its instability across datasets. Finally, DepictQA-Wild demonstrates superior performance across both settings by a large margin, showcasing its substantial advantage.

Quantitative results of assessment reasoning and comparison reasoning are shown in Tab. V and Tab. VI. First, the performance of the VLM-specific models significantly declines on tasks outside their defined scopes. For instance, Co-Instruct’s performance is unsatisfactory on full-reference tasks. Second, GPT-4V shows robust reasoning abilities, stably outperforming prior IQA-specific VLMs. Third, DepictQA-Wild surpasses GPT-4V, especially in the non-reference setting, affirming its superior reasoning abilities. Finally, DepictQA-Wild achieves relatively good GPT-4 score and ROUGE-L, indicative of the overall semantic accuracy, but a low BLEU score (yet remains much higher than GPT-4V), which reflects word-level consistency. This suggests that while our predicted answers do not precisely duplicate the ground truths word-for-word, they preserve similar meanings with diverse expressions.

Qualitative results of our model on the four tasks in the non-reference setting are depicted in Fig. 2. More qualitative results are provided in Figs. S4 to S8 of *Supp. Mat.*

TABLE V: **Assessment reasoning and comparison reasoning results** with GPT-4 score metric in the full-reference / non-reference setting. The best results are marked in **bold**.

Methods	Assessment Reasoning		Comparison Reasoning	
	Single-dist.	Multi-dist.	Single-dist.	Multi-dist.
GPT-4V	67.8 / 59.2	71.0 / 62.3	66.2 / 60.3	67.2 / 60.1
Q-Instruct	- / 45.7	- / 45.8	-	-
Co-Instruct	40.1 / 45.3	41.9 / 46.7	37.6 / 48.1	35.6 / 48.0
DepictQA-Wild	76.8 / 74.2	75.6 / 72.3	75.1 / 74.9	71.7 / 68.7

C. Quality score regression

Our key focus in this work is to *generate descriptive language rather than quality scores*. We focus more on linguistic descriptions because language is an effective interaction tool in an LLM-based intelligent agent. With the rapid development of LLMs and multi-modal techniques, in an LLM-based intelligent agent, language could be a useful tool for interacting and communicating across quality-related tasks such as image assessment, refinement, editing, and recommendation. Still, if it is required, our approach can produce quality scores.

Quality score regression. The score regression results are evaluated on the PIPAL, KADID, TID2013, and CSIQ datasets. These datasets include high-quality reference images and their distorted versions under various distortions. We calculate the win rate of an image against others to determine its quality score. Specifically, for an image A, we randomly sample comparison candidates, such as B, C, D, *etc.*, which share the same content as A but have different distortions. Image A is then compared pairwise with each

TABLE VI: **Assessment reasoning and comparison reasoning results** with classical metrics (BLEU and ROUGE-L) in the full-reference / non-reference setting. The best results are **bold**.

Methods	Assessment Reasoning				Comparison Reasoning			
	Single-distortion		Multi-distortion		Single-distortion		Multi-distortion	
	BLEU	ROUGE-L	BLEU	ROUGE-L	BLEU	ROUGE-L	BLEU	ROUGE-L
GPT-4V	0.020/0.010	0.248/0.224	0.023/0.015	0.246/0.223	0.029/0.025	0.261/0.243	0.030/0.024	0.251/0.238
Q-Instruct	- / 0.003	- / 0.210	- / 0.002	- / 0.198	-	-	-	-
Co-Instruct	0.008/0.005	0.201/0.204	0.002/0.003	0.209/0.203	0.039/0.041	0.239/0.234	0.034/0.036	0.239/0.234
Ours	0.132/0.129	0.423/0.422	0.180/0.170	0.420/0.415	0.207/0.207	0.466/0.463	0.176/0.172	0.420/0.413

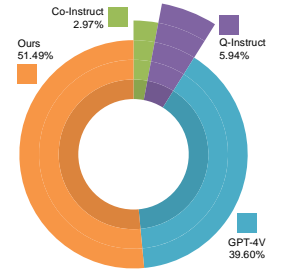


Fig. 7: User study results.

TABLE VII: **Results of quality score regression** with SRCC / PLCC metrics. The best results are emphasized in **bold**.

(a) Full-reference setting.				
Methods	PIPAL ^{test}	KADID ^{test}	TID2013	CSIQ
SSIM	0.624 / 0.680	0.750 / 0.751	0.746 / 0.802	0.861 / 0.857
FSIM	0.673 / 0.746	0.855 / 0.857	0.841 / 0.875	0.937 / 0.937
LPIPS	0.639 / 0.718	0.799 / 0.803	0.798 / 0.851	0.905 / 0.926
DepictQA-Wild	0.743 / 0.780	0.938 / 0.943	0.852 / 0.886	0.934 / 0.949
(b) Non-reference setting.				
Methods	PIPAL ^{test}	KADID ^{test}	TID2013	CSIQ
NIQE	0.300 / 0.367	0.430 / 0.499	0.315 / 0.413	0.660 / 0.747
CLIPQA	0.448 / 0.491	0.644 / 0.653	0.616 / 0.690	0.761 / 0.798
MUSIQ	0.539 / 0.570	0.650 / 0.668	0.578 / 0.693	0.755 / 0.811
MANIQA	0.558 / 0.602	0.482 / 0.527	0.472 / 0.603	0.701 / 0.714
DepictQA-Wild	0.742 / 0.778	0.937 / 0.941	0.847 / 0.866	0.912 / 0.938

of its comparison candidates (B, C, D, *etc.*). Finally, the win rate of Image A against all its compared candidates is calculated as its quality score. The comparison numbers per image for PIPAL, KADID, TID2013, and CSIQ datasets are 58, 62, 60, and 15, respectively. We show that the comparison number per image could be reduced significantly without large performance degradation in Tab. S3 of *Supp. Mat.* The results of quality score regression are given in Tab. VII and Tab. VII, proving that our method can generate accurate quality scores.

Assessing in-the-wild images with different contents. Existing real-world IQA datasets like KonIQ [98] and SPAQ [99] contain real distorted images with various contents. To regress quality scores from such a dataset, our model needs to compare images with different contents though *it is trained only to compare images with similar contents*, as shown in Task 2 of Fig. 2. The results in Tab. VIII show that even with a task gap between training and test, our original DepictQA-Wild still achieves comparable results with previous score-based IQA methods in score regression. Furthermore, we formulate real-world IQA datasets into instant rating tasks to re-train our DepictQA-Wild, *i.e.*, trained on KonIQ then evaluated on SPAQ, and vice versa. Our re-trained DepictQA-Wild outperforms all baselines trained on the same dataset. These results indicate that our method is capable of assessing in-the-wild images with different contents.

Results on Q-Bench. Q-Bench [4] is a VLM benchmark for low-level perception, but it mainly contains multiple-choice questions, whereas our model targets descriptive assessments, making direct evaluation mismatched. To test whether our data still helps on Q-Bench, we co-train with the multiple-choice dataset Q-Instruct [5] in Tab. XI. Co-training on Q-Instruct and our dataset consistently outperforms training on Q-Instruct

TABLE VIII: **Results of quality score calculation on SPAQ and KonIQ datasets** with SRCC / PLCC metrics. The best results are **bold**. DepictQA-Wild needs to *compare images with different contents* to obtain the quality score, since all images in the two datasets contain different contents. The original DepictQA-Wild is only trained to compare images with similar contents, which brings a task gap. When trained on the same dataset as baselines, DepictQA-Wild surpasses the baseline methods.

(a) Results on SPAQ dataset.						
Methods	NIQE	CLIPQA	MUSIQ	MANIQA	Ours	Ours
Train Set	-	-	KonIQ	KonIQ	KonIQ	Original
SRCC	0.664	0.700	0.856	0.755	0.859	0.835
PLCC	0.679	0.722	0.859	0.765	0.861	0.841

(b) Results on KonIQ dataset.						
Methods	NIQE	CLIPQA	DBCNN	MUSIQ	Ours	Ours
Train Set	-	-	SPAQ	SPAQ	SPAQ	Original
SRCC	0.530	0.685	0.731	0.753	0.787	0.717
PLCC	0.533	0.717	0.758	0.680	0.807	0.729

TABLE IX: **Our assistant model** surpasses GPT-4V in *instant rating* task. The metric is accuracy in the full-reference / non-reference setting. The best results are highlighted in **bold**.

	TID2013	LIVE-MD	MDID2013
GPT-4V	84.4 / 88.1	79.6 / 72.7	70.6 / 67.6
Our Assistant Model	94.9 / 94.6	93.1 / 92.8	90.1 / 89.8

alone, especially in distortion-related questions, demonstrating the benefit of our dataset even under a format shift. We borrow LLaVA results trained on Q-Instruct from [5] for reference.

D. Ablation Studies

Relationships between the comparison reasoning and instant rating tasks are studied in Tab. X. First, comparison reasoning task improves the performance on four instant rating datasets, but decreases the results on two datasets. Overall, comparison reasoning task helps the instant rating. Second, instant rating task stably improves the performance on comparison reasoning task.

Confidence. We examine the correlation between the performance and estimated confidence in Fig. 9. For *distortion identification* and *instant rating* tasks, across both full-reference and non-reference settings, our model demonstrates improved performance as the confidence interval increases. This validates the effectiveness of our confidence estimation.

Assistant model. To construct *comparison reasoning* responses, we train an assistant model to predict comparison

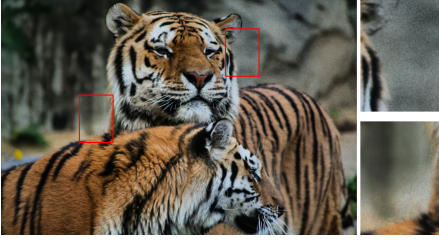


Fig. 8: One example of model-restored image by SwinIR [100].

TABLE X: Relationships between the comparison reasoning and instant rating tasks. The best results are **bold**. Overall, the two tasks are beneficial to each other.

(a) Results on the instant rating task.						
	BAPPS ^{test}	KADID ^{test}	PIPAL ^{test}	TID2013	LIVE-MD	MDID2013
Only Rating	81.6 / 81.6	92.4 / 92.3	89.1 / 89.0	94.2 / 94.1	92.9 / 92.7	92.1 / 91.7
Co-training	84.7 / 82.4	93.6 / 93.1	90.5 / 90.0	96.9 / 96.4	92.1 / 91.8	90.0 / 89.6

(b) Results on the comparison reasoning task.						
	Single-distortion			Multi-distortion		
	GPT-4 Score	BLEU	ROUGE-L	GPT-4 Score	BLEU	ROUGE-L
Only Reasoning	74.3 / 69.6	0.203 / 0.202	0.465 / 0.453	70.6 / 69.1	0.165 / 0.165	0.414 / 0.407
Co-training	75.1 / 74.9	0.207 / 0.207	0.466 / 0.463	71.7 / 68.7	0.176 / 0.172	0.420 / 0.413

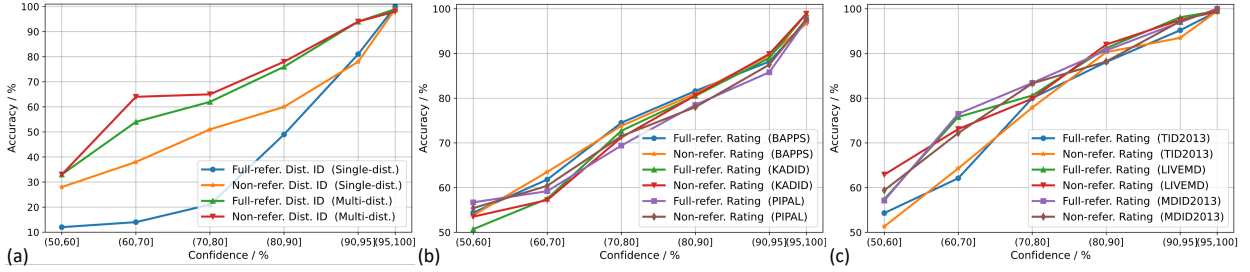


Fig. 9: Our estimated confidence scores are high correlated to the model performance on (a) distortion identification and (b) (c) instant rating tasks on different benchmarks in both full-reference and non-reference settings.

TABLE XI: Results on Q-Bench [4]. The best results are highlighted in **bold**.

Q-Bench	Yes-or-No	What	How	Distortion	Other
LLaVA (Q-Instruct trained)	66.4	58.2	50.5	49.4	65.7
Ours (Q-Instruct trained)	70.5	49.6	51.7	55.4	56.7
Ours (Q-Instruct + Our data trained)	74.0	62.8	54.0	66.7	63.9

results (see Fig. 3). These results serve as pseudo labels, which are subsequently provided to GPT-4V to generate responses. We compare the assistant model to GPT-4V on three out-of-distribution IQA datasets. The results in Tab. IX affirm the superiority of the assistant model.

Retaining resolution. In Tab. XII, we study the effects of retaining resolution. Specially, we randomly sample 1,000 high-quality images whose aspect ratios are greater than 4 : 3. These images are either resized by swapping their height and width (denoted as $H \leftrightarrow W$), or bi-linearly down-sampled by a scale factor of 0.5, 0.75, 0.8, 0.85, 0.9, or 0.95. DepictQA-Wild is requested to conduct the *instant rating* task, i.e., compare the original and resized images to determine the superior one. The alternative method of retaining resolution is to resize both original image and resized image to a larger resolution, which can maintain the quality difference. In contrast, resizing both images to smaller resolution results in two nearly same images. The results are presented in Tab. XII. First, retaining resolution is crucial for identifying images with better aspect ratio or higher resolution. Second, with down-sampling becomes severer (i.e., aspect ratio is from 0.95 to 0.5), the accuracy is improved since the quality drop is more significant. Third, for severe down-sampling (e.g., aspect ratio is 0.5) where the quality degradation is quite obviously, retaining resolution or just resizing both images to a larger size both perform well ($\geq 99.0\%$). Finally, however, for relatively slight down-sampling (e.g., aspect ratio is from 0.75 to 0.95), the performance of retaining resolution is stably superior than resizing.

TABLE XII: Retaining resolution during both training and inference is important to identify images with better aspect ratio or higher resolution.

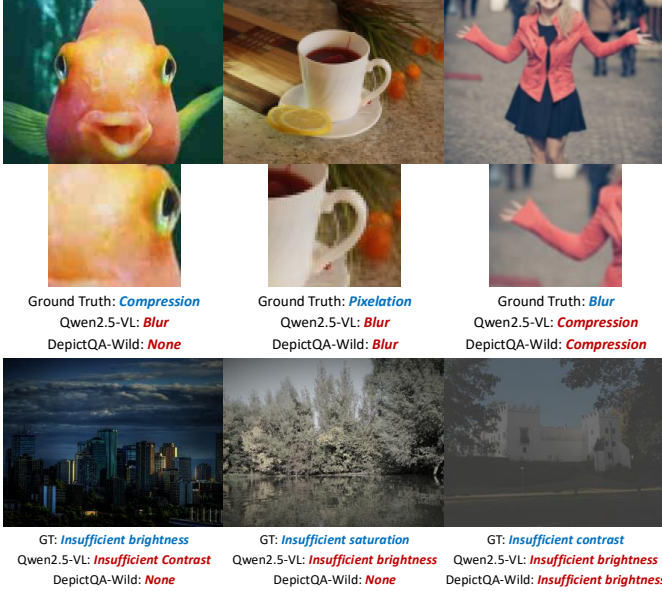
Retain Resolution?		H \leftrightarrow W	0.5 \times	0.75 \times	0.8 \times	0.85 \times	0.9 \times	0.95 \times
Training	Inference							
\times	\times	73.0	99.0	93.5	91.7	83.8	77.2	71.2
\checkmark	\times	85.6	99.8	99.4	99.0	95.9	94.8	89.4
\checkmark	\checkmark	98.8	99.9	99.6	99.3	99.1	96.8	97.0

Ablation study on module choice. Under the same VLM architecture framework and the same training loss, we compare two vision-text connectors (i.e., vision abstractor v.s. projector) and three LLMs on distortion identification and instant rating tasks. The default vision-text connector and LLM in this ablation study are vision projector and Vicuna-v1.5-7B. The results in Tab. XIII show that simply replacing vision-text connectors or LLMs has relatively little influence on performance. Considering that vision abstractor can greatly reduce the computational burden than projector, we select abstractor by default. For example, for a 448×448 image, projector generates 1024 tokens, while abstractor only outputs 64 tokens. Note that the computation amount is proportional to the square of the number of tokens.

Ablation on comparison order. We evaluate the impact of comparison order using the fine-grained dataset of [101], following its protocol to report *consistency* / *accuracy* / *correlation*. Here, *consistency* measures prediction stability when the two input images are swapped. As shown in Tab. XIV, our model attains $>90\%$ consistency under order reversal, and achieves substantially higher comparison accuracy and score correlation than Q-Instruct and GPT-4V. The Q-Instruct and GPT-4V results are quoted from [101]. These findings indicate that our model is robust to input-order variations. In addition, we provide the average confidence of our model in Tab. XV. The results show that the confidence of consistent

TABLE XIII: **Simply replacing modules** (*i.e.*, vision-text connectors and LLMs) has relatively little influence on performance.

Types	Architectures	Distortion Identification		Instant Rating					
		Single-dist. ID	Multi-dist. ID	BAPPS ^{test}	KADID ^{test}	PIPAL ^{test}	TID2013	LIVE-MD	MDID2013
Vision-text connector	Projector	97.9 / 94.7	90.5 / 89.5	82.7 / 81.4	92.7 / 92.4	89.2 / 88.8	96.2 / 95.9	92.1 / 91.9	89.1 / 88.4
	Abstractor	97.7 / 94.1	91.3 / 89.3	84.7 / 82.4	93.6 / 93.1	90.5 / 90.0	96.9 / 96.4	92.1 / 91.8	90.0 / 89.6
LLM	Vicuna-v1.5-7B	97.9 / 94.7	90.5 / 89.5	82.7 / 81.4	92.7 / 92.4	89.2 / 88.8	96.2 / 95.9	92.1 / 91.9	89.1 / 88.4
	Vicuna-v0-7B	96.9 / 93.6	89.8 / 89.3	82.5 / 81.3	92.8 / 92.2	88.2 / 88.1	95.0 / 94.7	91.2 / 91.1	90.5 / 90.2
	LLaMA-2-7B	97.0 / 94.0	90.6 / 89.1	81.7 / 81.5	92.6 / 92.0	88.4 / 87.9	94.6 / 94.1	91.8 / 91.1	90.9 / 90.7

Fig. 10: **Failure cases** where the model confuses some similar distortions, leading to misclassification.TABLE XIV: **Ablation results of comparison order** on fine-grained dataset released in [101]. We follow [101] to report the consistency (%) / accuracy (%) / correlation as metrics. The best results are highlighted in **bold**.

	Q-Instruct [66]	GPT-4V [2]	DepictQA-Wild
CSIQ (Levels)	11.5 / 8.1 / 0.557	41.9 / 40.2 / 0.906	95.5 / 92.5 / 0.958
CSIQ (Types)	11.7 / 6.9 / 0.416	32.5 / 24.4 / 0.482	90.5 / 69.0 / 0.857
SPAQ (Scores)	44.8 / 23.3 / 0.328	65.3 / 39.8 / 0.448	92.1 / 59.6 / 0.961

predictions is substantially higher than that of inconsistent ones, highlighting the model’s ability for self-evaluation.

Failure cases. We further examine typical failure cases for a general VLM (*i.e.*, Qwen2.5-VL-7B) and our DepictQA-Wild. Both models sometimes confuse visually similar distortions. In the first row of Fig. 10, they misclassify “compression” (blocky artifacts), “pixelation” (aliasing-induced jaggedness), and “blur” (low-frequency smoothing). In the second row, they confuse “insufficient brightness”, “insufficient saturation”, and “insufficient contrast”, which also produce similar global appearance changes. These results suggest that the fine-grained discrimination ability of current models remains limited.

E. Real-world Applications

Assessing web-downloaded images. A practical usage of an IQA model involves assessing the quality of real images. We collect a total of 50 real-world images from the web,

TABLE XV: **Confidence estimation** of consistent and inconsistent comparison results on fine-grained dataset in [101].

Confidence statistics	Consistency	Inconsistency
CSIQ (Levels)	0.933 ± 0.120	0.629 ± 0.083
CSIQ (Types)	0.860 ± 0.141	0.611 ± 0.098
SPAQ (Scores)	0.900 ± 0.125	0.649 ± 0.110

TABLE XVI: **Results on model-processed images.** The best results are **bold**. GPT-4V exhibits variability in ranking, so its results are reported as mean \pm standard deviation.

	NIQE	ClipIQA	MUSIQ	ManIQA	GPT-4V	Ours
Rank \downarrow	2.20	1.40	1.60	1.80	1.34 ± 0.27	1.20
Accuracy \uparrow	45.5	72.7	77.3	66.4	74.5	82.7

featuring diverse contents including animals, plants, faces, buildings, and landscapes. Qualitative results in Fig. 11 and Fig. S8 (in *Supp. Mat.*) indicate that our method can assess real images with detailed descriptions. More importantly, DepictQA-Wild can describe how the distortions affect the contents. For example, in Fig. 11d, our model first accurately identifies the “severe quantization”, then describes that the quantization “causes banding in the sky and water”, and finally concludes that the quality “is considerably degraded”. We also conduct a user study with 20 participants involved. Participants are instructed to choose the assessment result that is of the highest quality among the test methods. The results are shown in Fig. 7, revealing that our approach stably outperforms baseline methods in aligning human perception.

Comparison on model-processed images. To develop image restoration models, one often needs to compare the restoration quality of different models. We consider five common image restoration tasks: super-resolution, denoising, JPEG compression artifact removal, motion deblurring, and defocus deblurring. For each task, we collect three to four cutting-edged models in recent years (listed in Tab. XVII), apply them to a correspondingly degraded image, and then manually rank the resultant model-processed images. To find the image considered best by VLMs, we linearly scan the candidates and compare them in pairs. As VLMs’ results are not deterministic and may be sensitive to the presentation order of images, we repeat the linear scan 10 times and randomly shuffle the scan order each time. The average rank of the found best restoration and the accuracy of the paired comparison are reported in Tab. XVI. First, DepictQA-Wild achieves an average rank of 1.20 (1 is the best), outperforming both GPT-4V and score-based methods. Second, though the temperature is set to 0, GPT-4V shows variability with a large standard deviation. Third, model-restored images are generally out-of-distribution for our model, while DepictQA-Wild exhibits

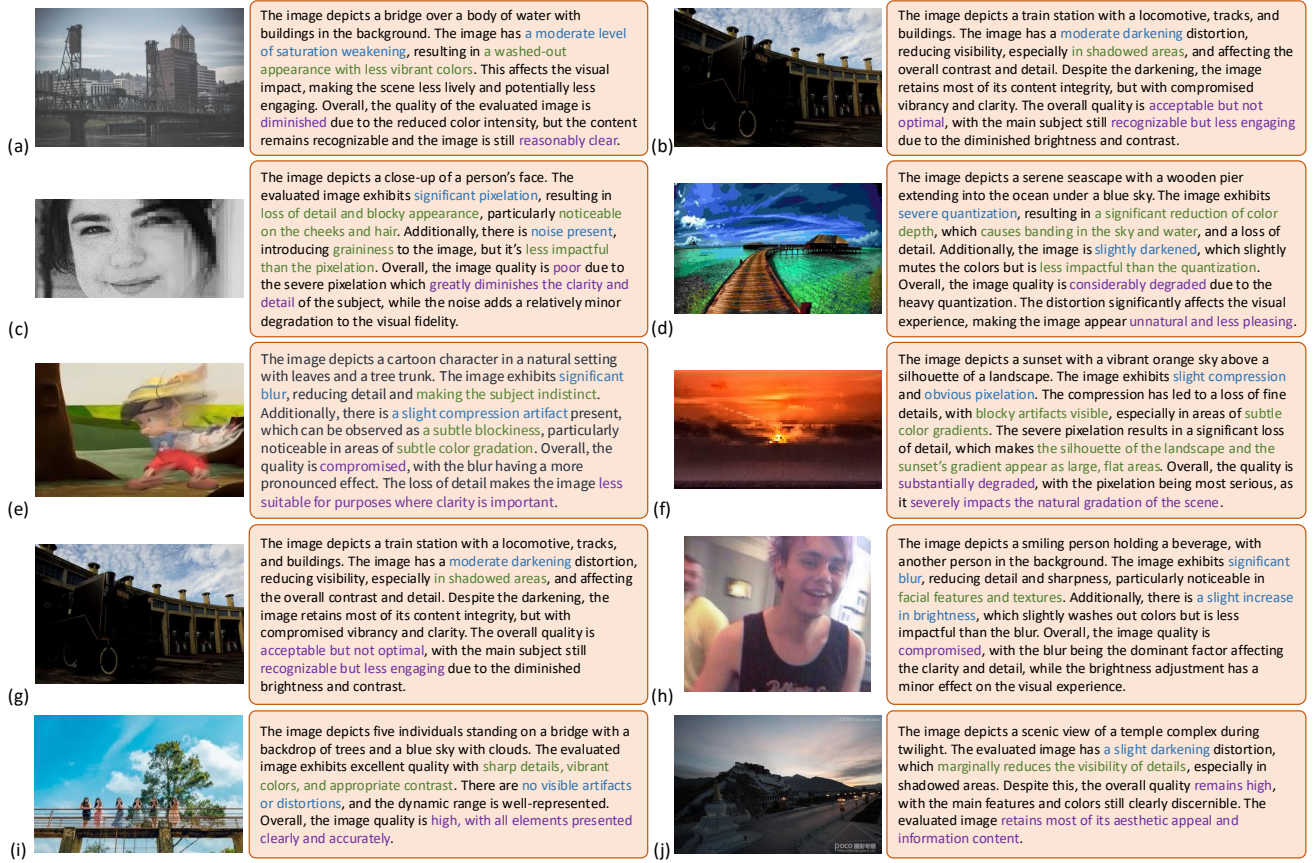


Fig. 11: **Qualitative results** on assessing web-downloaded images. More results in Fig. S8 of *Supp. Mat.*

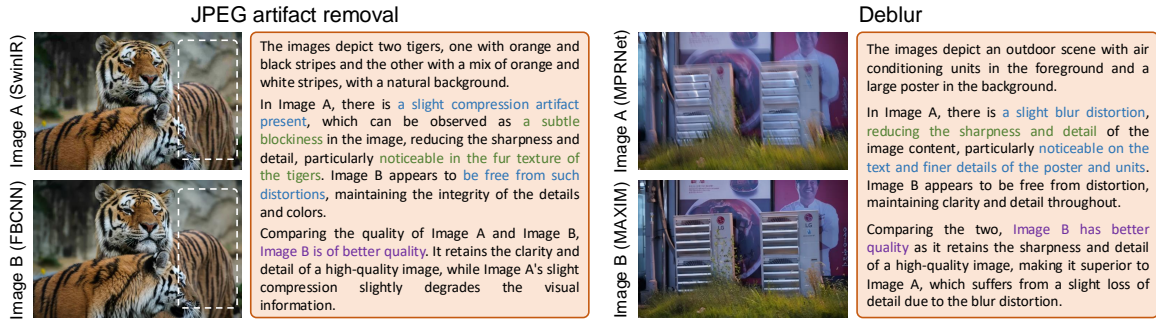


Fig. 12: **Qualitative results** of detailed comparison reasoning on model-processed images.

excellent generalization ability on these images. For example, the image in Fig. 8 is restored from a noisy image. There is still remnant noise, which is somewhat strange. For such an OOD image, our DepictQA-Wild correctly recognizes it to be inferior, but MANIQA, MUSIQ, and NIQE consider it as the best of the four candidates. Finally, we provide two qualitative results of detailed comparison reasoning on model-processed images in Fig. 12. One compares SwinIR and FBCNN in the JPEG compression artifact removal task, and the other compares MPRNet and MAXIM in the deblur task. Our model can generate a reasonable explanation for the comparison results.

F. Complexity and Efficiency

Training cost. The total parameters are 7.11B, including 6.76B for LLM, 0.30B for vision encoder, and 54M for vision

TABLE XVII: **Image restoration models** used in real-world experiments of comparing model-processed images, including SwinIR [100], HAT [102], X-Restormer [103], MPRNet [104], Restormer [105], FBCNN [106], MAXIM [107], MPRNet [104], DRBNet [108], and IFAN [109]. For FBCNN, “ $q=90$ ” means training on the quality factor 90, and “blind” means blind to the quality factor.

Image restoration task	Image restoration models
Super-resolution	SwinIR, HAT, X-Restormer
Denosing	SwinIR, MPRNet, Restormer, X-Restormer
JPEG artifact removal	SwinIR, FBCNN ($q=90$), FBCNN (blind)
Motion deblurring	MAXIM, MPRNet, Restormer
Defocus deblurring	DRBNet, IFAN, Restormer

abstractor. The trainable parameters are 70M (54M for vision abstractor and 16M for LoRA), constituting only 0.98% of the total parameters. The model is trained on 8 GPUs (RTX

A6000). The training is completed in around 22 hours.

Inference cost. The inference latency depends on the response length and it is tested on a single RTX A6000 GPU. For brief tasks with the short answer prompt (about 2.92 words), the inference time stands at approximately 2.23s / batch=32, transformed to 0.07s / sample. For the assessment reasoning task (75.84 words on average), the inference time is 22.97s / batch=32 (*i.e.*, 0.72s per response). Despite adopting VLMs, our DepictQA-Wild remains deployable on a single consumer GPU (*e.g.*, RTX3090).

VI. CONCLUSIONS AND LIMITATIONS

We introduce DepictQA-Wild, a VLM-based IQA model, empowered by a new multi-functional task paradigm, dataset enrichment, and training technique, surpassing baseline methods in both benchmarks and two real-world applications, showing the potential of descriptive quality assessment.

Limitations. First, the fine-grained abilities requiring more high-level perception skills are still unsatisfactory. For example, in Fig. 11c, though identifying noise and pixelation successfully, our model fails to point out that they are respectively located in the left and right parts. One solution is to take the segmentation model to add various distortions to different regions. Second, for the convenience of evaluating, analyzing, and improving the model, we mainly focus on standardized answers. To achieve more flexible responses, LLM rewriting and human annotation can be used to increase linguistic diversity during dataset construction. Third, whether our assessment can be used as feedback to improve the quality of generation or restoration models is still under-explored.

REFERENCES

- [1] H. Liu, C. Li, Q. Wu, and Y. J. Lee, "Visual instruction tuning," in *Proceedings of the Annual Conference on Neural Information Processing Systems*, vol. 36, 2023, pp. 34 892–34 916.
- [2] OpenAI, "GPT-4V(ision) system card," 2023. [Online]. Available: <https://openai.com/research/gpt-4v-system-card>
- [3] Q. Ye, H. Xu, J. Ye, M. Yan, A. Hu, H. Liu, Q. Qian, J. Zhang, and F. Huang, "mPLUG-Owl2: Revolutionizing multi-modal large language model with modality collaboration," in *Proceedings of the IEEE/CVF Conference on Computer Vision and Pattern Recognition*, 2024, pp. 13 040–13 051.
- [4] H. Wu, Z. Zhang, E. Zhang, C. Chen, L. Liao, A. Wang, C. Li, W. Sun, Q. Yan, G. Zhai *et al.*, "Q-Bench: A benchmark for general-purpose foundation models on low-level vision," in *Proceedings of the International Conference on Learning Representations*, 2024.
- [5] H. Wu, Z. Zhang, E. Zhang, C. Chen, L. Liao, A. Wang, K. Xu, C. Li, J. Hou, G. Zhai *et al.*, "Q-Instruct: Improving low-level visual abilities for multi-modality foundation models," in *Proceedings of the IEEE/CVF Conference on Computer Vision and Pattern Recognition*, 2024, pp. 25 490–25 500.
- [6] H. Wu, H. Zhu, Z. Zhang, E. Zhang, C. Chen, L. Liao, C. Li, A. Wang, W. Sun, Q. Yan *et al.*, "Towards open-ended visual quality comparison," in *Proceedings of the European Conference on Computer Vision*, 2024, pp. 360–377.
- [7] T. Wu, K. Ma, J. Liang, Y. Yang, and L. Zhang, "A comprehensive study of multimodal large language models for image quality assessment," in *Proceedings of the European Conference on Computer Vision*, 2024, pp. 143–160.
- [8] Z. You, Z. Li, J. Gu, Z. Yin, T. Xue, and C. Dong, "Depicting beyond scores: Advancing image quality assessment through multi-modal language models," in *Proceedings of the European Conference on Computer Vision*, 2024, pp. 259–276.
- [9] N. Ponomarenko, L. Jin, O. Ieremeiev, V. Lukin, K. Egiazarian, J. Astola, B. Vozel, K. Chehdi, M. Carli, F. Battisti *et al.*, "Image database TID2013: Peculiarities, results and perspectives," *Signal Processing: Image Communication*, 2015.
- [10] R. Zhang, P. Isola, A. A. Efros, E. Shechtman, and O. Wang, "The unreasonable effectiveness of deep features as a perceptual metric," in *Proceedings of the IEEE/CVF Conference on Computer Vision and Pattern Recognition*, 2018, pp. 586–595.
- [11] J. Ke, Q. Wang, Y. Wang, P. Milanfar, and F. Yang, "MUSIQ: Multi-scale image quality transformer," in *Proceedings of the IEEE/CVF International Conference on Computer Vision*, 2021, pp. 5148–5157.
- [12] G. Jinjin, C. Haoming, C. Haoyu, Y. Xiaoxing, J. S. Ren, and D. Chao, "PIPAL: A large-scale image quality assessment dataset for perceptual image restoration," in *Proceedings of the European Conference on Computer Vision*, 2020, pp. 633–651.
- [13] H. R. Sheikh and A. C. Bovik, "Image information and visual quality," *IEEE Transactions on Image Processing*, vol. 15, no. 2, pp. 430–444, 2006.
- [14] Z. Wang, A. C. Bovik, H. R. Sheikh, and E. P. Simoncelli, "Image quality assessment: from error visibility to structural similarity," *IEEE Transactions on Image Processing*, vol. 13, no. 4, pp. 600–612, 2004.
- [15] L. Zhang, L. Zhang, X. Mou, and D. Zhang, "FSIM: A feature similarity index for image quality assessment," *IEEE Transactions on Image Processing*, vol. 20, no. 8, pp. 2378–2386, 2011.
- [16] E. Prashnani, H. Cai, Y. Mostofi, and P. Sen, "PieAPP: Perceptual image-error assessment through pairwise preference," in *Proceedings of the IEEE Conference on Computer Vision and Pattern Recognition*, 2018, pp. 1808–1817.
- [17] S. Bosse, D. Maniry, K.-R. Müller, T. Wiegand, and W. Samek, "Deep neural networks for no-reference and full-reference image quality assessment," *IEEE Transactions on Image Processing*, vol. 27, no. 1, pp. 206–219, 2017.
- [18] Y. Cao, Z. Wan, D. Ren, Z. Yan, and W. Zuo, "Incorporating semi-supervised and positive-unlabeled learning for boosting full reference image quality assessment," in *Proceedings of the IEEE/CVF Conference on Computer Vision and Pattern Recognition*, 2022, pp. 5851–5861.
- [19] K. Ding, K. Ma, S. Wang, and E. P. Simoncelli, "Image quality assessment: Unifying structure and texture similarity," *IEEE Transactions on Pattern Analysis and Machine Intelligence*, vol. 44, no. 5, pp. 2567–2581, 2020.
- [20] K. Ding, Y. Liu, X. Zou, S. Wang, and K. Ma, "Locally adaptive structure and texture similarity for image quality assessment," in *Proceedings of the ACM International Conference on Multimedia*, 2021, pp. 2483–2491.
- [21] A. Ghildyal and F. Liu, "Shift-tolerant perceptual similarity metric," in *Proceedings of the European Conference on Computer Vision*, 2022, pp. 91–107.
- [22] G. Yin, W. Wang, Z. Yuan, C. Han, W. Ji, S. Sun, and C. Wang, "Content-variant reference image quality assessment via knowledge distillation," in *Proceedings of the AAAI Conference on Artificial Intelligence*, vol. 36, no. 3, 2022, pp. 3134–3142.
- [23] W. Zhou and Z. Wang, "Quality assessment of image super-resolution: Balancing deterministic and statistical fidelity," in *Proceedings of the ACM International Conference on Multimedia*, 2022, pp. 934–942.
- [24] C. Ma, C.-Y. Yang, X. Yang, and M.-H. Yang, "Learning a no-reference quality metric for single-image super-resolution," *Computer Vision and Image Understanding*, vol. 158, pp. 1–16, 2017.
- [25] A. Mittal, A. K. Moorthy, and A. C. Bovik, "No-reference image quality assessment in the spatial domain," *IEEE Transactions on Image Processing*, vol. 21, no. 12, pp. 4695–4708, 2012.
- [26] A. Mittal, R. Soundararajan, and A. C. Bovik, "Making a "completely blind" image quality analyzer," *IEEE Signal Processing Letters*, vol. 20, no. 3, pp. 209–212, 2012.
- [27] A. K. Moorthy and A. C. Bovik, "A two-step framework for constructing blind image quality indices," *IEEE Signal Processing Letters*, vol. 17, no. 5, pp. 513–516, 2010.
- [28] —, "Blind image quality assessment: From natural scene statistics to perceptual quality," *IEEE Transactions on Image Processing*, vol. 20, no. 12, pp. 3350–3364, 2011.
- [29] M. A. Saad, A. C. Bovik, and C. Charrier, "Blind image quality assessment: A natural scene statistics approach in the dct domain," *IEEE Transactions on Image Processing*, vol. 21, no. 8, pp. 3339–3352, 2012.
- [30] H. Tang, N. Joshi, and A. Kapoor, "Learning a blind measure of perceptual image quality," in *Proceedings of the IEEE/CVF Conference on Computer Vision and Pattern Recognition*, 2011, pp. 305–312.
- [31] L. Kang, P. Ye, Y. Li, and D. Doermann, "Convolutional neural networks for no-reference image quality assessment," in *Proceedings of the IEEE/CVF Conference on Computer Vision and Pattern Recognition*, 2014, pp. 1733–1740.

- [32] X. Liu, J. Van De Weijer, and A. D. Bagdanov, "RankIQA: Learning from rankings for no-reference image quality assessment," in *Proceedings of the IEEE/CVF International Conference on Computer Vision*, 2017, pp. 1040–1049.
- [33] D. Pan, P. Shi, M. Hou, Z. Ying, S. Fu, and Y. Zhang, "Blind predicting similar quality map for image quality assessment," in *Proceedings of the IEEE/CVF Conference on Computer Vision and Pattern Recognition*, 2018, pp. 6373–6382.
- [34] S. Su, Q. Yan, Y. Zhu, C. Zhang, X. Ge, J. Sun, and Y. Zhang, "Blindly assess image quality in the wild guided by a self-adaptive hyper network," in *Proceedings of the IEEE/CVF Conference on Computer Vision and Pattern Recognition*, 2020, pp. 3667–3676.
- [35] S. Sun, T. Yu, J. Xu, W. Zhou, and Z. Chen, "GraphIQA: Learning distortion graph representations for blind image quality assessment," *IEEE Transactions on Multimedia*, vol. 25, pp. 2912–2925, 2022.
- [36] H. Zheng, H. Yang, J. Fu, Z.-J. Zha, and J. Luo, "Learning conditional knowledge distillation for degraded-reference image quality assessment," in *Proceedings of the IEEE/CVF International Conference on Computer Vision*, 2021, pp. 10242–10251.
- [37] H. Zhu, L. Li, J. Wu, W. Dong, and G. Shi, "MetaIQA: Deep meta-learning for no-reference image quality assessment," in *Proceedings of the IEEE/CVF Conference on Computer Vision and Pattern Recognition*, 2020, pp. 14 143–14 152.
- [38] J. Wang, K. C. Chan, and C. C. Loy, "Exploring CLIP for assessing the look and feel of images," in *Proceedings of the AAAI Conference on Artificial Intelligence*, vol. 37, no. 2, 2023, pp. 2555–2563.
- [39] S. Yang, T. Wu, S. Shi, S. Lao, Y. Gong, M. Cao, J. Wang, and Y. Yang, "MANIQA: Multi-dimension attention network for no-reference image quality assessment," in *Proceedings of the IEEE/CVF Conference on Computer Vision and Pattern Recognition*, 2022, pp. 1191–1200.
- [40] W. Zhang, D. Li, C. Ma, G. Zhai, X. Yang, and K. Ma, "Continual learning for blind image quality assessment," *IEEE Transactions on Pattern Analysis and Machine Intelligence*, vol. 45, no. 3, pp. 2864–2878, 2022.
- [41] W. Zhang, G. Zhai, Y. Wei, X. Yang, and K. Ma, "Blind image quality assessment via vision-language correspondence: A multitask learning perspective," in *Proceedings of the IEEE/CVF Conference on Computer Vision and Pattern Recognition*, 2023, pp. 14 071–14 081.
- [42] W.-L. Chiang, Z. Li, Z. Lin, Y. Sheng, Z. Wu, H. Zhang, L. Zheng, S. Zhuang, Y. Zhuang, J. E. Gonzalez *et al.*, "Vicuna: An open-source chatbot impressing GPT-4 with 90%* ChatGPT quality," 2023. [Online]. Available: <https://vicuna.lmsys.org>
- [43] OpenAI, "GPT-4 technical report," *arXiv preprint arXiv:2303.08774*, 2023.
- [44] H. Touvron, T. Lavril, G. Izacard, X. Martinet, M.-A. Lachaux, T. Lacroix, B. Rozière, N. Goyal, E. Hambro, F. Azhar *et al.*, "LLaMA: Open and efficient foundation language models," *arXiv preprint arXiv:2302.13971*, 2023.
- [45] J.-B. Alayrac, J. Donahue, P. Luc, A. Miech, I. Barr, Y. Hasson, K. Lenc, A. Mensch, K. Millican, M. Reynolds *et al.*, "Flamingo: A visual language model for few-shot learning," *Proceedings of the Annual Conference on Neural Information Processing Systems*, vol. 35, pp. 23 716–23 736, 2022.
- [46] W. Dai, J. Li, D. Li, A. Tiong, J. Zhao, W. Wang, B. Li, P. N. Fung, and S. Hoi, "InstructBLIP: Towards general-purpose vision-language models with instruction tuning," *Proceedings of the Annual Conference on Neural Information Processing Systems*, vol. 36, pp. 49 250–49 267, 2023.
- [47] H. Wei, L. Kong, J. Chen, L. Zhao, Z. Ge, J. Yang, J. Sun, C. Han, and X. Zhang, "Vary: Scaling up the vision vocabulary for large vision-language model," in *Proceedings of the European Conference on Computer Vision*, 2024, pp. 408–424.
- [48] Q. Ye, H. Xu, G. Xu, J. Ye, M. Yan, Y. Zhou, J. Wang, A. Hu, P. Shi, Y. Shi *et al.*, "mPLUG-Owl: Modularization empowers large language models with multimodality," *arXiv preprint arXiv:2304.14178*, 2023.
- [49] Z. Yin, J. Wang, J. Cao, Z. Shi, D. Liu, M. Li, X. Huang, Z. Wang, L. Sheng, L. Bai *et al.*, "LAMM: Language-assisted multi-modal instruction-tuning dataset, framework, and benchmark," in *Proceedings of the Annual Conference on Neural Information Processing Systems*, vol. 36, 2023, pp. 26 650–26 685.
- [50] P. Zhang, X. Dong, B. Wang, Y. Cao, C. Xu, L. Ouyang, Z. Zhao, S. Ding, S. Zhang, H. Duan, W. Zhang, H. Yan, X. Zhang, W. Li, J. Li, K. Chen, C. He, X. Zhang, Y. Qiao, D. Lin, and J. Wang, "InternLM-XComposer: A vision-language large model for advanced text-image comprehension and composition," *arXiv preprint arXiv:2309.15112*, 2023.
- [51] R. Zhang, J. Han, C. Liu, A. Zhou, P. Lu, Y. Qiao, H. Li, and P. Gao, "LLaMA-Adapter: Efficient fine-tuning of large language models with zero-initialized attention," in *Proceedings of the International Conference on Learning Representations*, 2024.
- [52] D. Zhu, J. Chen, X. Shen, X. Li, and M. Elhoseiny, "MiniGPT-4: Enhancing vision-language understanding with advanced large language models," in *Proceedings of the International Conference on Learning Representations*, 2024.
- [53] H. Agrawal, K. Desai, Y. Wang, X. Chen, R. Jain, M. Johnson, D. Batra, D. Parikh, S. Lee, and P. Anderson, "Nocaps: Novel object captioning at scale," in *Proceedings of the IEEE/CVF International Conference on Computer Vision*, 2019, pp. 8948–8957.
- [54] X. Chen, H. Fang, T.-Y. Lin, R. Vedantam, S. Gupta, P. Dollár, and C. L. Zitnick, "Microsoft COCO captions: Data collection and evaluation server," *arXiv preprint arXiv:1504.00325*, 2015.
- [55] P. Young, A. Lai, M. Hodosh, and J. Hockenmaier, "From image descriptions to visual denotations: New similarity metrics for semantic inference over event descriptions," *Transactions of the Association for Computational Linguistics*, vol. 2, pp. 67–78, 2014.
- [56] Y. Goyal, T. Khot, D. Summers-Stay, D. Batra, and D. Parikh, "Making the V in VQA matter: Elevating the role of image understanding in visual question answering," in *Proceedings of the IEEE/CVF Conference on Computer Vision and Pattern Recognition*, 2017, pp. 6904–6913.
- [57] Y. Liu, H. Duan, Y. Zhang, B. Li, S. Zhang, W. Zhao, Y. Yuan, J. Wang, C. He, Z. Liu *et al.*, "MMBench: Is your multi-modal model an all-around player?" in *Proceedings of the European Conference on Computer Vision*, 2024, pp. 216–233.
- [58] P. Lu, S. Mishra, T. Xia, L. Qiu, K.-W. Chang, S.-C. Zhu, O. Tafjord, P. Clark, and A. Kalyan, "Learn to explain: Multimodal reasoning via thought chains for science question answering," *Proceedings of the Annual Conference on Neural Information Processing Systems*, vol. 35, pp. 2507–2521, 2022.
- [59] A. Masry, X. L. Do, J. Q. Tan, S. Joty, and E. Hoque, "ChartQA: A benchmark for question answering about charts with visual and logical reasoning," in *Findings of the Association for Computational Linguistics*, 2022, pp. 2263–2279.
- [60] M. Mathew, D. Karatzas, and C. Jawahar, "DocVQA: A dataset for vqa on document images," in *Proceedings of the IEEE/CVF Winter Conference on Applications of Computer Vision*, 2021, pp. 2200–2209.
- [61] A. Singh, V. Natarajan, M. Shah, Y. Jiang, X. Chen, D. Batra, D. Parikh, and M. Rohrbach, "Towards VQA models that can read," in *Proceedings of the IEEE/CVF Conference on Computer Vision and Pattern Recognition*, 2019, pp. 8317–8326.
- [62] H. Zhu, X. Sui, B. Chen, X. Liu, P. Chen, Y. Fang, and S. Wang, "2AFC prompting of large multimodal models for image quality assessment," *IEEE Transactions on Circuits and Systems for Video Technology*, 2024.
- [63] H. Wu, Z. Zhang, W. Zhang, C. Chen, L. Liao, C. Li, Y. Gao, A. Wang, E. Zhang, W. Sun *et al.*, "Q-Align: teaching LLMs for visual scoring via discrete text-defined levels," in *Proceedings of the International Conference on Machine Learning*, 2024, pp. 54 015–54 029.
- [64] Z. You, X. Cai, J. Gu, T. Xue, and C. Dong, "Teaching large language models to regress accurate image quality scores using score distribution," in *Proceedings of the IEEE/CVF Conference on Computer Vision and Pattern Recognition*, 2025, pp. 14 483–14 494.
- [65] D. Guo, D. Yang, H. Zhang, J. Song, P. Wang, Q. Zhu, R. Xu, R. Zhang, S. Ma, X. Bi *et al.*, "DeepSeek-R1: Incentivizes reasoning in LLMs through reinforcement learning," *Nature*, vol. 645, no. 8081, pp. 633–638, 2025.
- [66] W. Li, X. Zhang, S. Zhao, Y. Zhang, J. Li, L. Zhang, and J. Zhang, "Q-Insight: Understanding image quality via visual reinforcement learning," in *Proceedings of the Annual Conference on Neural Information Processing Systems*, 2025.
- [67] Z. Shao, P. Wang, Q. Zhu, R. Xu, J. Song, X. Bi, H. Zhang, M. Zhang, Y. Li, Y. Wu *et al.*, "DeepSeekMath: Pushing the limits of mathematical reasoning in open language models," *arXiv preprint arXiv:2402.03300*, 2024.
- [68] T. Wu, J. Zou, J. Liang, L. Zhang, and K. Ma, "VisualQuality-R1: Reasoning-induced image quality assessment via reinforcement learning to rank," in *Proceedings of the Annual Conference on Neural Information Processing Systems*, 2025.
- [69] Z. Cai, J. Zhang, X. Yuan, P.-T. Jiang, W. Chen, B. Tang, L. Yao, Q. Wang, J. Chen, and B. Li, "Q-Ponder: A unified training pipeline for reasoning-based visual quality assessment," *arXiv preprint arXiv:2506.05384*, 2025.

- [70] A. B. Arrieta, N. Díaz-Rodríguez, J. Del Ser, A. Benetot, S. Tabik, A. Barbado, S. García, S. Gil-López, D. Molina, R. Benjamins *et al.*, “Explainable artificial intelligence (XAI): Concepts, taxonomies, opportunities and challenges toward responsible AI,” *Information Fusion*, vol. 58, pp. 82–115, 2020.
- [71] H. Chefer, S. Gur, and L. Wolf, “Transformer interpretability beyond attention visualization,” in *Proceedings of the IEEE/CVF Conference on Computer Vision and Pattern Recognition*, 2021, pp. 782–791.
- [72] Y. Hao, L. Dong, F. Wei, and K. Xu, “Self-attention attribution: Interpreting information interactions inside transformer,” in *Proceedings of the AAAI Conference on Artificial Intelligence*, vol. 35, no. 14, 2021, pp. 12 963–12 971.
- [73] R. Fu, Q. Hu, X. Dong, Y. Guo, Y. Gao, and B. Li, “Axiom-based Grad-CAM: Towards accurate visualization and explanation of CNNs,” *arXiv preprint arXiv:2008.02312*, 2020.
- [74] P. Schramowski, W. Stammer, S. Teso, A. Brugger, F. Herbert, X. Shao, H.-G. Luigs, A.-K. Mahlein, and K. Kersting, “Making deep neural networks right for the right scientific reasons by interacting with their explanations,” *Nature Machine Intelligence*, vol. 2, no. 8, pp. 476–486, 2020.
- [75] Y. Shen, B. Sheng, R. Fang, H. Li, L. Dai, S. Stolte, J. Qin, W. Jia, and D. Shen, “Domain-invariant interpretable fundus image quality assessment,” *Medical Image Analysis*, vol. 61, p. 101654, 2020.
- [76] B. Jo, D. Cho, I. K. Park, and S. Hong, “IFQA: Interpretable face quality assessment,” in *Proceedings of the IEEE/CVF Winter Conference on Applications of Computer Vision*, 2023, pp. 3444–3453.
- [77] P. Costa, A. Campilho, B. Hooi, A. Smailagic, K. Kitani, S. Liu, C. Faloutsos, and A. Galdran, “EyeQual: Accurate, explainable, retinal image quality assessment,” in *IEEE International Conference on Machine Learning and Applications (ICMLA)*, 2017, pp. 323–330.
- [78] Y. Hu, B. Liu, J. Kasai, Y. Wang, M. Ostendorf, R. Krishna, and N. A. Smith, “TIFA: Accurate and interpretable text-to-image faithfulness evaluation with question answering,” in *Proceedings of the IEEE/CVF International Conference on Computer Vision*, 2023, pp. 20 406–20 417.
- [79] H. Lin, V. Hosu, and D. Saupe, “DeepFL-IQA: Weak supervision for deep iqa feature learning,” *arXiv preprint arXiv:2001.08113*, 2020.
- [80] —, “KADID-10k: A large-scale artificially distorted iqa database,” in *Proceedings of the International Conference on Quality of Multimedia Experience (QoMEX)*, 2019, pp. 1–3.
- [81] D. Jayaraman, A. Mittal, A. K. Moorthy, and A. C. Bovik, “Objective quality assessment of multiply distorted images,” in *Proceedings of the Asilomar Conference on Signals, Systems and Computers (ASILOMAR)*, 2012, pp. 1693–1697.
- [82] W. Sun, F. Zhou, and Q. Liao, “MDID: A multiply distorted image database for image quality assessment,” *Pattern Recognition*, vol. 61, pp. 153–168, 2017.
- [83] A. Radford, J. W. Kim, C. Hallacy, A. Ramesh, G. Goh, S. Agarwal, G. Sastry, A. Askell, P. Mishkin, J. Clark *et al.*, “Learning transferable visual models from natural language supervision,” in *Proceedings of the International Conference on Machine Learning*, 2021, pp. 8748–8763.
- [84] R. A. Frazor and W. S. Geisler, “Local luminance and contrast in natural images,” *Vision Research*, vol. 46, no. 10, pp. 1585–1598, 2006.
- [85] D. Hasler and S. E. Suesstrunk, “Measuring colorfulness in natural images,” in *Human Vision and Electronic Imaging VIII*, vol. 5007, 2003, pp. 87–95.
- [86] P. J. Bex, S. G. Solomon, and S. C. Dakin, “Contrast sensitivity in natural scenes depends on edge as well as spatial frequency structure,” *Journal of Vision*, vol. 9, no. 10, pp. 1–19, 2009.
- [87] A. Hyvärinen, J. Hurri, and P. O. Hoyer, *Natural image statistics: A probabilistic approach to early computational vision*. Springer Science & Business Media, 2009, vol. 39.
- [88] H. Liu, C. Li, Y. Li, B. Li, Y. Zhang, S. Shen, and Y. J. Lee, “LLaVA-NeXT: Improved reasoning, ocr, and world knowledge,” 2024. [Online]. Available: <https://llava-vl.github.io/blog/2024-01-30-llava-next/>
- [89] T. Kudo and J. Richardson, “SentencePiece: A simple and language independent subword tokenizer and detokenizer for neural text processing,” in *Proceedings of the Conference on Empirical Methods in Natural Language Processing: System Demonstrations*, 2018, pp. 66–71.
- [90] E. J. Hu, P. Wallis, Z. Allen-Zhu, Y. Li, S. Wang, L. Wang, W. Chen *et al.*, “LoRA: Low-Rank adaptation of large language models,” in *Proceedings of the International Conference on Learning Representations*, 2022.
- [91] J. Duan, H. Cheng, S. Wang, A. Zavalny, C. Wang, R. Xu, B. Kailkhura, and K. Xu, “Shifting attention to relevance: Towards the predictive uncertainty quantification of free-form large language models,” in *Proceedings of the Annual Meeting of the Association for Computational Linguistics*, 2024, pp. 5050–5063.
- [92] N. Reimers and I. Gurevych, “Sentence-BERT: Sentence embeddings using siamese bert-networks,” in *Proceedings of the Conference on Empirical Methods in Natural Language Processing and the International Joint Conference on Natural Language Processing (EMNLP-IJCNLP)*, 2019, pp. 3982–3992.
- [93] A. See, P. J. Liu, and C. D. Manning, “Get to the point: Summarization with pointer-generator networks,” in *Proceedings of the Annual Meeting of the Association for Computational Linguistics*, 2017, pp. 1073–1083.
- [94] A. Vaswani, N. Shazeer, N. Parmar, J. Uszkoreit, L. Jones, A. N. Gomez, Ł. Kaiser, and I. Polosukhin, “Attention is all you need,” *Proceedings of the Annual Conference on Neural Information Processing Systems*, vol. 30, 2017.
- [95] X. An, Y. Xie, K. Yang, W. Zhang, X. Zhao, Z. Cheng, Y. Wang, S. Xu, C. Chen, C. Wu *et al.*, “LLaVA-OneVision-1.5: Fully open framework for democratized multimodal training,” *arXiv preprint arXiv:2509.23661*, 2025.
- [96] Z. Chen, W. Wang, Y. Cao, Y. Liu, Z. Gao, E. Cui, J. Zhu, S. Ye, H. Tian, Z. Liu *et al.*, “Expanding performance boundaries of open-source multimodal models with model, data, and test-time scaling,” *arXiv preprint arXiv:2412.05271*, 2024.
- [97] S. Bai, K. Chen, X. Liu, J. Wang, W. Ge, S. Song, K. Dang, P. Wang, S. Wang, J. Tang *et al.*, “Qwen2.5-VL technical report,” *arXiv preprint arXiv:2502.13923*, 2025.
- [98] V. Hosu, H. Lin, T. Sziranyi, and D. Saupe, “KonIQ-10k: An ecologically valid database for deep learning of blind image quality assessment,” *IEEE Transactions on Image Processing*, vol. 29, pp. 4041–4056, 2020.
- [99] Y. Fang, H. Zhu, Y. Zeng, K. Ma, and Z. Wang, “Perceptual quality assessment of smartphone photography,” in *Proceedings of the IEEE/CVF Conference on Computer Vision and Pattern Recognition*, 2020, pp. 3677–3686.
- [100] J. Liang, J. Cao, G. Sun, K. Zhang, L. Van Gool, and R. Timofte, “SwinIR: Image restoration using swin transformer,” in *Proceedings of the IEEE/CVF International Conference on Computer Vision*, 2021, pp. 1833–1844.
- [101] H. Zhu, X. Sui, B. Chen, X. Liu, P. Chen, Y. Fang, and S. Wang, “2AFC prompting of large multimodal models for image quality assessment,” *IEEE Transactions on Circuits and Systems for Video Technology*, 2024.
- [102] X. Chen, X. Wang, J. Zhou, Y. Qiao, and C. Dong, “Activating more pixels in image super-resolution transformer,” in *Proceedings of the IEEE/CVF Conference on Computer Vision and Pattern Recognition*, 2023, pp. 22 367–22 377.
- [103] X. Chen, Z. Li, Y. Pu, Y. Liu, J. Zhou, Y. Qiao, and C. Dong, “A comparative study of image restoration networks for general backbone network design,” in *Proceedings of the European Conference on Computer Vision*, 2024, pp. 74–91.
- [104] S. W. Zamir, A. Arora, S. Khan, M. Hayat, F. S. Khan, M.-H. Yang, and L. Shao, “Multi-stage progressive image restoration,” in *Proceedings of the IEEE/CVF Conference on Computer Vision and Pattern Recognition*, 2021, pp. 14 821–14 831.
- [105] S. W. Zamir, A. Arora, S. Khan, M. Hayat, F. S. Khan, and M.-H. Yang, “Restormer: Efficient transformer for high-resolution image restoration,” in *Proceedings of the IEEE/CVF Conference on Computer Vision and Pattern Recognition*, 2022, pp. 5728–5739.
- [106] J. Jiang, K. Zhang, and R. Timofte, “Towards flexible blind jpeg artifacts removal,” in *Proceedings of the IEEE/CVF International Conference on Computer Vision*, 2021, pp. 4997–5006.
- [107] Z. Tu, H. Talebi, H. Zhang, F. Yang, P. Milanfar, A. Bovik, and Y. Li, “MAXIM: Multi-axis mlp for image processing,” in *Proceedings of the IEEE/CVF Conference on Computer Vision and Pattern Recognition*, 2022, pp. 5769–5780.
- [108] L. Ruan, B. Chen, J. Li, and M. Lam, “Learning to deblur using light field generated and real defocus images,” in *Proceedings of the IEEE/CVF Conference on Computer Vision and Pattern Recognition*, 2022, pp. 16 304–16 313.
- [109] J. Lee, H. Son, J. Rim, S. Cho, and S. Lee, “Iterative filter adaptive network for single image defocus deblurring,” in *Proceedings of the IEEE/CVF Conference on Computer Vision and Pattern Recognition*, 2021, pp. 2034–2042.

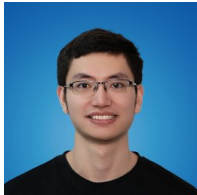


Zhiyuan You is a Ph.D. candidate from Multimedia Laboratory at The Chinese University of Hong Kong, under the supervision of Prof. Chao Dong and Prof. Tianfan Xue. He obtained both his Bachelor's and Master's degrees from Shanghai Jiao Tong University, where he was supervised by Prof. Xinyi Le and Prof. Yu Zheng. His research interests focus on low-level vision based on foundation models.



industrial applications of machine learning.

Jinjin Gu received his Ph.D. degree from the School of Electrical and Computer Engineering at the University of Sydney in 2024, under the supervision of Prof. Wanli Ouyang and Prof. Luping Zhou. Prior to that, he earned a Bachelor's degree in Computer Science and Engineering from The Chinese University of Hong Kong, Shenzhen, in 2020. He collaborates closely with Prof. Chao Dong and Prof. Junhua Zhao. His research focuses on computer vision and image processing, with additional interests in the interpretability of deep learning algorithms and the



Xin Cai received the B.S. degree in computer science from University of Chinese Academy of Sciences (UCAS) in 2020 and the M.S. degree from the Institute of Computing Technology (ICT), Chinese Academy of Sciences (CAS), Beijing, China. He is currently pursuing the Ph.D. degree in The Chinese University of Hong Kong (CUHK). His research interests include computer vision, computational photography and machine learning.



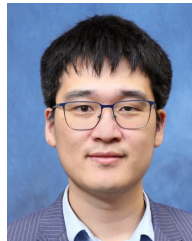
Zheyuan Li is currently a Ph.D. Student at University of Macau. He has also worked as a research intern since 2021 in Shenzhen Institutes of Advanced Technology, Chinese Academy of Sciences. He received his B.E. degree from Northwestern Polytechnical University, Xi'an, in 2022. His research interests include image super-resolution, image restoration and enhancement, and multi-modal low-level-vision model.



Kaiwen Zhu is currently a Ph.D. student in Shanghai Jiao Tong University supervised by Prof. Chao Dong. He obtained his B.Eng. degree from Shanghai Jiao Tong University in 2024. He has been working as an intern researcher in Shanghai Artificial Intelligence Laboratory since 2023. His research focuses on low-level vision and intelligent agents.



Chao Dong is a professor at Shenzhen Institutes of Advanced Technology, Chinese Academy of Science (SIAT), and Shanghai Artificial Intelligence Laboratory. In 2014, he first introduced deep learning method – SRCNN into the super-resolution field. This seminal work was chosen as one of the top ten “Most Popular Articles” of TPAMI in 2016. His team has won several championships in international challenges –NTIRE2018, PIRM2018, NTIRE2019, NTIRE2020 AIM2020 and NTIRE2022. He worked in SenseTime from 2016 to 2018, as the team leader of Super-Resolution Group. In 2021, he was chosen as one of the World's Top 2% Scientists. In 2022, he was recognized as the AI 2000 Most Influential Scholar Honorable Mention in computer vision. His current research interest focuses on low-level vision problems, such as image/video super-resolution, denoising and enhancement.



Tianfan Xue is a Vice-Chancellor Assistant Professor at the Multimedia Lab in the Department of Information Engineering at the Chinese University of Hong Kong (CUHK). Prior to this, he worked in the Computational Photography Team at Google Research for over five years. He received his Ph.D. degree from the Computer Science and Artificial Intelligence Laboratory (CSAIL) at MIT in 2017. He also holds an M.Phil. degree from CUHK, obtained in 2011, and a Bachelor's degree from Tsinghua University. His research focuses on computational photography, 3D reconstruction, and generation. His work on bilateral based 3D reconstruction has won SIGGRAPH Honorable mention 2024. He also served as an area chair for WACV, CVPR, NeurIPS, and ACM MM.

APPENDIX

A. Dataset Details

1) *Details of Distortion Library:* As stated in Sec. III-B, to facilitate the dataset construction, we design and implement a comprehensive distortion library. Our distortion system contains 12 distortion super-categories in total, with each category consisting of multiple sub-categories. For instance, the “blur” category encompasses “Gaussian blur”, “motion blur”, “lens blur”, *etc.* In total, there are 35 sub-categories. For each sub-category, there are 5 severity levels: “slight”, “moderate”, “obvious”, “serious”, and “catastrophic”. In this section, we elaborate on our distortion implementations, including the principles, formulas, and severity setup. We also provide one example for each implementation in Fig. S3, with the reference image in Fig. S1.

Blur.

- Gaussian blur. The distorted image is generated by convolving the reference image with a Gaussian blur kernel. We set the kernel size (s_k) to be a function of the standard deviation (σ_k) of the blur kernel: $s_k = \text{round}(4 \times \sigma_k) + 1$.
- Motion blur. Linear motion blur is applied to the reference image using the linear filter, where $(r, \sigma) \in [(5, 3), (10, 5), (15, 7), (15, 9), (20, 12)]$.
- Glass blur. Filter the image using a Gaussian filter, then randomly jitter each pixel in the image by x pixels, and repeat this process n iterations. $[\sigma, x, n] \in [(0.7, 1, 1), (0.9, 2, 1), (1.2, 2, 2), (1.4, 3, 2), (1.6, 4, 2)]$.
- Lens blur. This distortion uses the circular average filter, where $r \in [1, 2, 4, 6, 8]$.
- Zoom blur. The image is gradually zoomed in and overlaid to calculate the average.
- Jitter blur. Each pixel is randomly displaced by a shift of $\text{randint}(-p, p)$ pixels both in x and y dimensions, with a total of 5 displacements, where $p \in [1, 2, 3, 4, 5]$.

Noise.

- Gaussian noise in RGB space. Additive Gaussian noise is applied to each of the RGB channels of an image, where $\sigma \in [0.05, 0.1, 0.15, 0.2, 0.25]$.
- Gaussian noise in YCrCb space. Similar to the Gaussian noise in RGB space, this distortion is implemented in YCbCr space, where the value of $(\sigma_l, \sigma_r, \sigma_b)$ can be $(0.05, 1, 1)$, $(0.06, 1.45, 1.45)$, $(0.07, 1.9, 1.9)$, $(0.08, 2.35, 2.35)$, or $(0.09, 2.8, 2.8)$.
- Speckle noise. Speckle Noise is also known as Multiplicative Gaussian noise, where $\sigma \in [0.14, 0.21, 0.28, 0.35, 0.42]$.
- Spatially correlated noise. The reference image is first corrupted by an additive Gaussian noise, which results in each pixel being corrupted by an independent and identically distributed noise pattern. The resultant image is then filtered with an average filter of kernel size 3×3 , correlating the intensity of each pixel with those of the neighboring pixels. More specifically, the distorted image is given by:

$$I_D(x, y, c) = \frac{1}{|N_n|} \sum_{i \in N_n} (I_R(x_i, y_i, c_i) + N(x_i, y_i, c_i)),$$



Fig. S1: **Reference image** for distorted images in Fig. S3.

where I_D is the distorted image, I_R is the reference image, N_n is the set of neighboring pixels, and $N(x, y, c) \sim \mathcal{N}(0, \sigma_g^2)$.

- Poisson noise. This distortion generates Poisson noise based on the image pixel values, where *intervals* $\in [80, 60, 40, 25, 15]$.
- Impulse noise. Impulse noise is also known as salt and pepper noise. The density of the noise: $d \in [0.01, 0.03, 0.05, 0.07, 0.10]$.

Compression.

- JPEG. The distorted image is a JPEG-compressed version of the reference image, where the parameter in Pillow, quality $q \in [25, 18, 12, 8, 5]$.
- JPEG 2000. This distortion is an advanced compression widely used, where the Pillow’s parameter quality $q \in [29, 27.5, 26, 24.5, 23]$.

Brightness.

- Brightness shift in HSV space. The RGB image is mapped to HSV, and then we enhance and reduce the brightness by V channel, where $\sigma \in [0.1, 0.2, 0.3, 0.4, 0.5]$ for Brightening and $\sigma \in [-0.1, -0.2, -0.3, -0.4, -0.5]$ for darkening.
- Brightness shift in RGB space. We enhance and reduce the brightness in all channels, where $\sigma \in [0.1, 0.15, 0.2, 0.27, 0.35]$ for Brightening and $\sigma \in [-0.1, -0.15, -0.2, -0.27, -0.35]$ for darkening.
- Gamma brightness tuning in HSV space. The RGB image is mapped to HSV space and then we enhanced and reduce the brightness by V channel with a gamma function, where $\gamma \in [0.7, 0.58, 0.47, 0.36, 0.25]$ for brightening and $\gamma \in [1.5, 1.8, 2.2, 2.7, 3.5]$ for darkening.

Contrast.

- Contrast tuning by scaling. Given an input image I_{in} , there is a corresponding I_{mean} , which is a gray image in which each element is the mean of I_{mean} . The distorted image I_D is generated as following: $I_D = I_{mean} * (1.0 - \alpha) + I_{in} * \alpha$, where $\alpha \in [0.75, 0.6, 0.45, 0.3, 0.2]$ for strengthening and $\alpha \in [1.4, 1.7, 2.1, 2.6, 4.0]$ for weakening.
- Contrast tuning by stretching. Contrast changing is performed as follows: $I_D(x, y, c) = 1 / (1 + (\frac{I_C}{I_R(x, y, c) + \epsilon})\alpha)$, where I_D is the distorted image, I_R is the reference image, and \bar{I}_C is the mean intensity for channel c .

$\alpha \in [1.0, 0.9, 0.8, 0.6, 0.4]$ for weakening, and $\alpha \in [2.0, 4.0, 6.0, 8.0, 10.0]$ for strengthening.

Saturate.

- Saturate tuning in HSV space. The reference image is firstly mapped into HSV space and then the S channel is scaled, where the scale factor $s \in [0.7, 0.55, 0.4, 0.2, 0.0]$ for weakening and $s \in [3.0, 6.0, 12.0, 20.0, 64.0]$ for enhancement.
- Saturate tuning in YCbCr space. The reference image I_R is firstly mapped into YCbCr space and then the distorted image I_D is generated like the following formulation:

$$I_D(x, y, Cb) = 128 + (I_R(x, y, Cb) - 128) \times s, \quad (S1)$$

$$I_D(x, y, Cr) = 128 + (I_R(x, y, Cr) - 128) \times s, \quad (S2)$$

where $s \in [0.6, 0.4, 0.2, 0.1, 0.0]$ donates the scale factor for weakening and $s \in [2.0, 3.0, 5.0, 8.0, 16.0]$ for strengthening.

Over-sharpen. The reference image I_R is firstly processed by a Gaussian blur kernel to generated a blurred image I_{blur} . Then the original image is over-sharpened with `cv2.addWeighted($I_R, 1 + \alpha, I_{blur}, -\alpha, 0$)`, where $\alpha \in [2, 2.8, 4, 6, 8]$.

Pixelate. The reference image is firstly down-sampled in BOX mode, then up-sampled to the original resolution in NEAREST mode, where the down-sampling factor $\sigma \in [0.5, 0.4, 0.3, 0.25, 0.2]$.

Quantize.

- Color quantization using histogram equalization. The color elements are divided into an equal histogram for quantization, where the number of classes $c \in [24, 16, 8, 6, 4]$.
- Color quantization using histogram median. This distortion is implemented by the function `PIL.Image.Quantize.MEDIANCUT`, where the number of classes $c \in [20, 15, 10, 6, 3]$.
- Color quantization using OTSU method, which is implemented by existing function `skimage.filters.threshold_multiotsu` to generate thresholds. The number of classes $c \in [15, 11, 8, 5, 3]$.

Multi-distortion setups. As discussed in Sec. III-B, multi-distortions may occur simultaneously on the same image in practical usage. First, we observe that humans can identify at most two distortions when three or more are applied, as in Fig. S2, thus we limit the number of applied distortions to two. Second, some distortions could weaken each other's presentation (e.g., "brighten" weakens "darken", "blur" weakens "over-sharpen"). Also, certain distortions show similar visual effects (e.g., "pixelate" looks similar to "blur"), making it hard to identify both if applied simultaneously. Hence, to exclude contradictory or similar distortion combinations, we manually review all possible combinations. All feasible distortion combinations are provided in Tab. S1.

Out-of-distribution setups. In Tab. III, we evaluate our model in an out-of-distribution (OOD) setting. Specifically, for a particular category of distortion (e.g., noise), we use some sub-categories (e.g., Poisson noise) during training, and

different sub-categories (e.g., impulse noise) for evaluation. Here we provide a detailed split of training distortions and evaluation distortions in Tab. S2.

2) *Details of Template pool:* As stated in Sec. III-C, for brief tasks, the questions and answers are templated and sampled from a pool. The questions of detailed tasks are also sampled from a pool. The question pools and answer pools (if possible) of *distortion identification*, *instant rating*, *assessment reasoning*, and *comparison reasoning* tasks are given in Tab. S4, Tab. S6, Tab. S5, and Tab. S7, respectively.

B. More Ablation Studies

Influence of comparison numbers. We calculate the win rate of one image over other compared images as the quality score. Here the compared images are selected by round robin for a small number, and random sampling for a large number. For the SPAQ dataset, the number of possible compared images is quite large, thus we adopt the random sampling strategy. The influence of comparison numbers is investigated in Tab. S3. It is shown that the comparison number could be reduced significantly without large performance degradation. In the most extreme cases (i.e., the comparison number is 1 or 2), we use the estimated confidence as weights to calculate the win rate as quality score. Otherwise, the values of the win rate are too discrete (i.e., the values of the win rate can only be 0 or 1 when the comparison number is 1). The results of our DepictQA-Wild are still reasonable in such extreme cases. Considering that the random sampling may bring large randomness or variance, we average the results with 5 random runs for small comparison numbers (i.e., < 10). Although the comparison number is small and the sampling process is random, our method is still very stable with relatively small standard deviations in Tab. S3.

C. More Qualitative Results

More qualitative results of *assessment reasoning*, *comparison reasoning*, and assessment on web-downloaded images are presented in Fig. S4, Fig. S5, Fig. S6, Fig. S7, and Fig. S8, respectively. Our DepictQA-Wild could accurately identify distortions, analyze their impacts on the display of image contents, then weigh the advantages and disadvantages of different aspects, and finally draw a final conclusion.

TABLE S1: **Multi-distortion setting** where we show all feasible distortion combinations.

First Distortion	All Possible Second Distortions
Blur	Brighten, Compression, Contrast Strengthen, Contrast Weaken, Darken, Noise, Quantize, Saturate Strengthen, Saturate Weaken
Brighten	Blur, Compression, Noise, Pixelate, Quantize
Compression	Blur, Brighten, Contrast Strengthen, Contrast Weaken, Darken, Noise, Saturate Strengthen, Saturate Weaken
Contrast Strengthen	Blur, Compression, Noise, Pixelate, Quantize
Contrast Weaken	Blur, Compression, Noise, Pixelate, Quantize
Darken	Blur, Compression, Noise, Pixelate, Quantize
Noise	Blur, Brighten, Compression, Contrast Strengthen, Contrast Weaken, Darken, Over-sharpen, Pixelate, Saturate Strengthen, Saturate Weaken
Over-sharpen	Brighten
Pixelate	Brighten, Contrast Strengthen, Contrast Weaken, Darken, Noise, Over-sharpen, Quantize, Saturate Strengthen, Saturate Weaken
Quantize	Brighten, Contrast Strengthen, Contrast Weaken, Darken, Noise, Over-sharpen, Pixelate, Saturate Strengthen, Saturate Weaken
Saturate Strengthen	Blur, Compression, Noise, Over-sharpen, Pixelate, Quantize
Saturate Weaken	Blur, Compression, Noise, Over-sharpen, Pixelate, Quantize

TABLE S2: **Setting of out-of-distribution (OOD) distortion identification.**

Category	Training distortions	Validation distortions
Blur	Motion blur, Glass blur, Lens blur, Zoom blur	Gaussian blur, Jitter blur
Noise	Gaussian noise in YCrCb space, Speckle noise, Spatial correlated noise, Poisson noise	Gaussian noise in RGB space, Impulse noise
Compression	JPEG compression	JPEG2000 compression
Brighten	Shift brighten in HSV & RGB spaces, Gamma brighten in HSV space	Gamma brighten in RGB space
Darken	Shift darken in HSV & RGB spaces, Gamma darken in HSV space	Gamma darken in RGB space
Contrast strengthen	Contrast strengthen by scaling	Contrast strengthen by stretching
Contrast weaken	Contrast weaken by scaling	Contrast weaken by stretching
Saturate strengthen	Saturate strengthen in HSV space	Saturate strengthen in YCrCb space
Saturate weaken	Saturate weaken in HSV space	Saturate weaken in YCrCb space
Quantization	Quantization by OTSU method, Quantization by histogram median	Quantization by histogram equalization

TABLE S3: **Influence of comparison numbers per image on SPAQ dataset** with SRCC and PLCC metrics. “(KONIQ)” means the model is trained on KONIQ dataset, which is also an in-the-wild IQA dataset. For small comparison numbers (< 10), we average the results with 5 random runs.

Comparison Numbers		100	50	25	10	5	2	1
DepictQA-Wild (Original)	SRCC	0.835	0.832	0.826	0.806	0.731 \pm 0.006	0.647 \pm 0.009	0.577 \pm 0.015
	PLCC	0.841	0.837	0.832	0.810	0.735 \pm 0.006	0.639 \pm 0.009	0.537 \pm 0.015
DepictQA-Wild (KONIQ)	SRCC	0.859	0.854	0.850	0.830	0.756 \pm 0.006	0.664 \pm 0.011	0.598 \pm 0.013
	PLCC	0.861	0.858	0.852	0.833	0.757 \pm 0.007	0.652 \pm 0.011	0.546 \pm 0.015

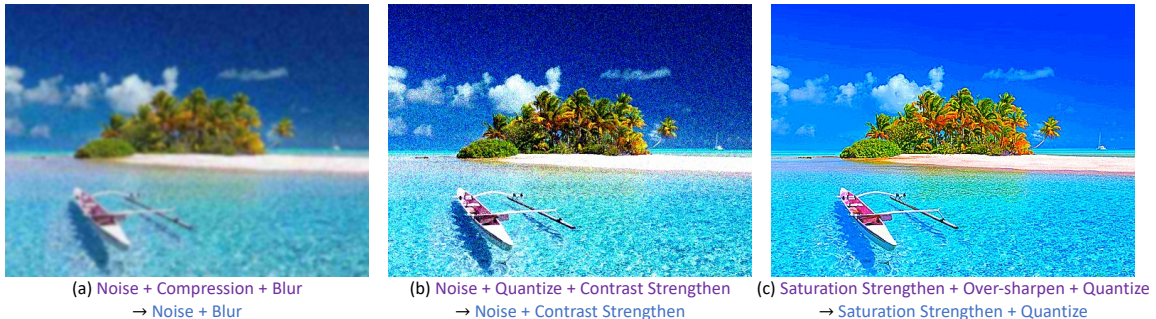


Fig. S2: Humans usually identify at most two distortions (blue) when three (purple) are applied.

TABLE S4: Question pool and answer pool of *distortion identification* task.

#	Question / Answer
1	Q: What are the primary degradation(s) observed in the evaluated image? A: The primary degradation(s) in the evaluated image is/are {}.
2	Q: What distortion(s) are most apparent in the evaluated image? A: The most apparent distortion(s) in the evaluated image is/are {}.
3	Q: Identify the chief degradation(s) in the evaluated image. A: The chief degradation(s) in the evaluated image is/are {}.
4	Q: Pinpoint the foremost image quality issue(s) in the evaluated image. A: The foremost image quality issue(s) is/are {}.
5	Q: What distortion(s) stand out in the evaluated image? A: The distortion(s) that stand out is/are {}.
6	Q: What distortion(s) are most prominent in the evaluated image? A: The most prominent distortion(s) is/are {}.
7	Q: What critical quality degradation(s) are present in the evaluated image? A: The critical quality degradation(s) presented is/are {}.
8	Q: Highlight the most significant distortion(s) in the evaluated image. A: The most significant distortion(s) in the evaluated image is/are {}.
9	Q: What distortion(s) most detrimentally affect the overall quality of the evaluated image? A: The distortion(s) that most detrimentally affect the overall quality is/are {}.
10	Q: Determine the most impactful distortion(s) in the evaluated image. A: The most impactful distortion(s) in the evaluated image is/are {}.
11	Q: Identify the most notable distortion(s) in the evaluated image's quality. A: The most notable distortion(s) in the evaluated image's quality is/are {}.
12	Q: What distortion(s) most significantly affect the evaluated image? A: The distortion(s) that most significantly affect the evaluated image is/are {}.
13	Q: Determine the leading degradation(s) in the evaluated image. A: The leading degradation(s) is/are {}.
14	Q: What distortion(s) are most prominent when examining the evaluated image? A: The most prominent distortion(s) is/are {}.
15	Q: What distortion(s) are most evident in the evaluated image? A: The most evident distortion(s) in the evaluated image is/are {}.
16	Q: What quality degradation(s) are most apparent in the evaluated image? A: The most apparent quality degradation(s) is/are {}.
17	Q: In terms of image quality, what are the most glaring issue(s) with the evaluated image? A: The most glaring issue(s) with the evaluated image is/are {}.
18	Q: What are the foremost distortion(s) affecting the evaluated image's quality? A: The foremost distortion(s) affecting the evaluated image's quality is/are {}.
19	Q: Identify the most critical distortion(s) in the evaluated image. A: The most critical distortion(s) is/are {}.
20	Q: In the evaluated image, what distortion(s) are most detrimental to image quality? A: In the evaluated image, {} is/are the most detrimental distortion(s) to image quality.
21	Q: What are the most severe degradation(s) observed in the evaluated image? A: The most severe degradation(s) is/are {}.
22	Q: What are the leading distortion(s) in the evaluated image? A: The leading distortion(s) in the evaluated image is/are {}.
23	Q: What are the most critical image quality issue(s) in the evaluated image? A: The most critical image quality issue(s) in the evaluated image is/are {}.
24	Q: What distortion(s) most notably affect the clarity of the evaluated image? A: The distortion(s) that most notably affect the clarity is/are {}.

TABLE S5: Question pool of *assessment reasoning* task.

#	Question
1	Could you assess the overall quality of the image and elaborate on your evaluation?
2	How would you rate the image's quality, and what factors contribute to your assessment?
3	Can you provide a detailed evaluation of the image's quality?
4	Please evaluate the image's quality and provide your reasons.
5	How do you perceive the quality of the image, and what aspects influence your judgment?
6	Offer an assessment of the image's quality, highlighting any strengths or weaknesses.
7	What is your opinion on the quality of the image? Explain your viewpoint.
8	Assess the quality of the image with detailed reasons.
9	How does the image's quality impact its overall effectiveness or appeal?
10	Evaluate the image's quality and justify your evaluation.
11	How about the overall quality of the image, and why?
12	Provide a thorough evaluation of the image's quality.
13	Examine the image's quality by considering factors influencing its clarity.
14	Analyze the image's quality, and detail your findings.
15	Provide a comprehensive assessment of the image's quality, including both strengths and areas for improvement.
16	Assess the image's quality from a professional standpoint.
17	Evaluate the image's clarity and explain how it contributes to the overall quality.
18	How would you rate the overall quality of the image, and why?
19	What is your opinion on the image's quality? Elaborate on your evaluation.
20	Evaluate the quality of the image and provide a comprehensive explanation.

TABLE S6: Question pool and answer pool of *instant rating* task.

#	Question / Answer
1	Q: Which image do you believe has better overall quality: Image A or Image B? A: I believe Image {} has better overall quality.
2	Q: Determine which image exhibits higher quality between Image A and Image B. A: In my assessment, Image {} exhibits higher quality.
3	Q: Compare the general quality of Image A and Image B, and state your preference. A: My preference leans towards Image {} to have better general quality.
4	Q: In your opinion, which image demonstrates superior quality: Image A or Image B? A: In my opinion, Image {} demonstrates superior quality.
5	Q: Which of the two images, Image A or Image B, do you consider to be of better quality? A: I consider Image {} to be of better quality.
6	Q: Evaluate the quality of Image A and Image B, and decide which one is superior. A: I conclude that Image {} is superior.
7	Q: Between Image A and Image B, which image do you think has better quality overall? A: I think Image {} has better quality overall.
8	Q: Determine which image, Image A or Image B, you perceive to have better quality. A: I determine that Image {} has better quality.
9	Q: Assess the quality of Image A and Image B, and choose the one you believe is superior. A: I choose Image {} to be superior in terms of quality.
10	Q: Which image stands out to you as having better quality: Image A or Image B? A: Image {} stands out as the superior choice in terms of quality.
11	Q: Can you compare the quality of Image A and Image B and decide which one is better? A: I find Image {} to be better after comparing the quality of both.
12	Q: Decide which image, Image A or Image B, you think possesses higher quality. A: I decide that Image {} possesses higher quality.
13	Q: Evaluate Image A and Image B, and select the one that you feel has better quality. A: Upon evaluation, I select Image {} as the one with better quality.
14	Q: Which of the two images, Image A or Image B, appears to have superior quality to you? A: To me, Image {} appears to have superior quality.
15	Q: Compare the quality of Image A and Image B, and determine which one you prefer. A: My preference leans towards Image {} after comparing the quality.
16	Q: Make a judgment on which image, Image A or Image B, you consider to be of better quality. A: I consider Image {} to be of better quality.
17	Q: Between Image A and Image B, which image do you perceive to have better quality overall? A: I perceive Image {} to have better quality overall.
18	Q: Assess the quality of Image A and Image B, and indicate which one you find to be better. A: I find Image {} emerges as the better option with superior quality.
19	Q: Which image, Image A or Image B, do you think displays better quality when compared? A: When compared, Image {} displays better quality.
20	Q: Differentiate between Image A and Image B in terms of overall quality and decide which one is superior. A: Image {} differentiates itself with superior quality.

TABLE S7: Question pool of *comparison reasoning* task.

#	Question
1	Compare the overall quality of Image A with Image B and provide a comprehensive explanation.
2	Which image has better visual quality, Image A or Image B? Can you explain the comparison results?
3	Evaluate the general visual appeal and quality of both Image A and Image B, and elaborate on which one excels.
4	Discuss the overall impression and quality of Image A versus Image B, and justify your assessment.
5	Compare the overall quality between Image A and Image B, and justify your comparison results.
6	Assess the overall visual quality of Image A and Image B, discussing which one delivers a more compelling visual quality.
7	Which image demonstrates higher overall quality, Image A or Image B? Please provide detailed reasoning for your evaluation.
8	Analyze the overall quality of both Image A and Image B, and explain which image stands out.
9	Compare the perceived quality of Image A with Image B, providing insights into their respective strengths and weaknesses.
10	Discuss the visual quality of Image A and Image B, and elaborate on which one appears more appealing.
11	Can you evaluate the overall quality in both Image A and Image B, and explain which one is superior?
12	Compare the overall visual impact and impression of Image A versus Image B, and justify your assessment of their quality.
13	Which image exhibits higher overall quality: Image A or Image B? Please explain your reasoning.
14	Evaluate the visual quality in Image A and Image B, providing insights into their comparative strengths.
15	Compare the overall quality between Image A and Image B, and discuss which one appears more appealing.
16	Assess the visual quality of both Image A and Image B, and explain which one is better.
17	Which image demonstrates superior quality: Image A or Image B? Please elaborate on your evaluation.
18	Discuss the overall impression of Image A versus Image B, and justify your assessment of their comparative quality.
19	Compare the visual quality of Image A with Image B, providing detailed insights into their respective strengths and weaknesses.
20	Evaluate the overall quality of Image A and Image B, and explain which one has higher quality.

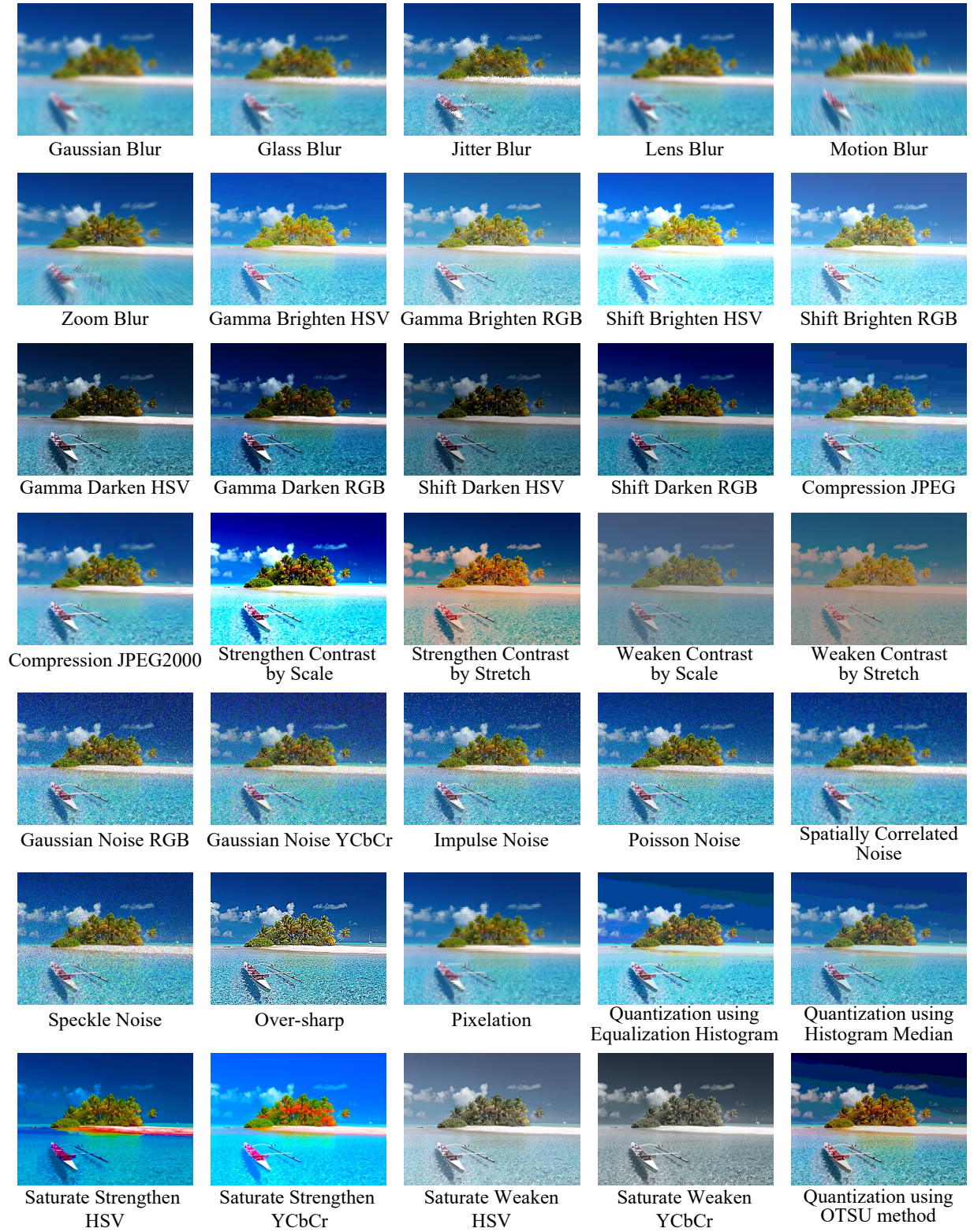


Fig. S3: **Distortion examples** of our distortion design. We showcase one example for each distortion implementation. The reference image is depicted in Fig. S1.

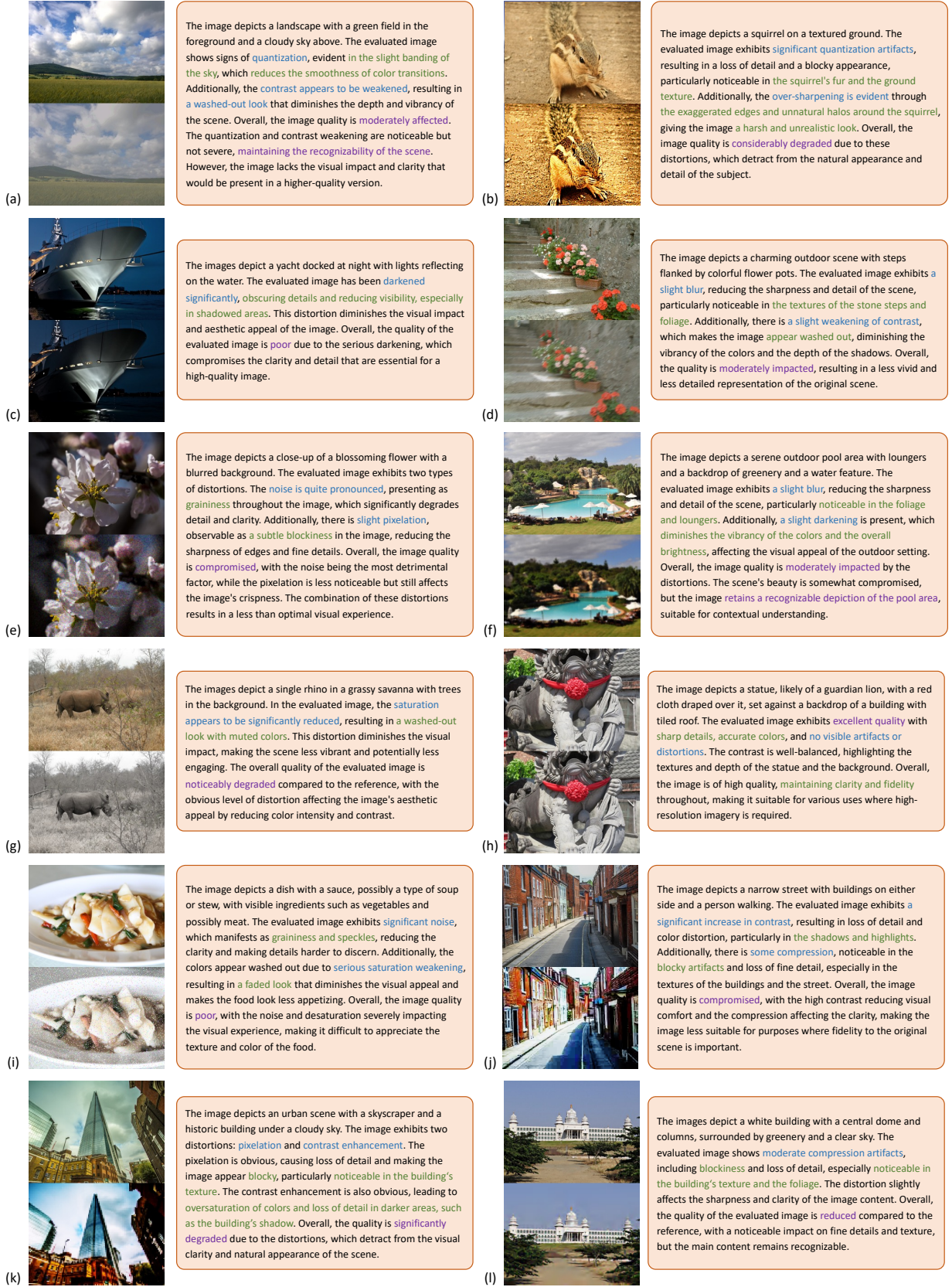


Fig. S4: **Qualitative results** on *assessment reasoning* task in the full-reference setting. The two images from top to down are the reference image and evaluated image, respectively.

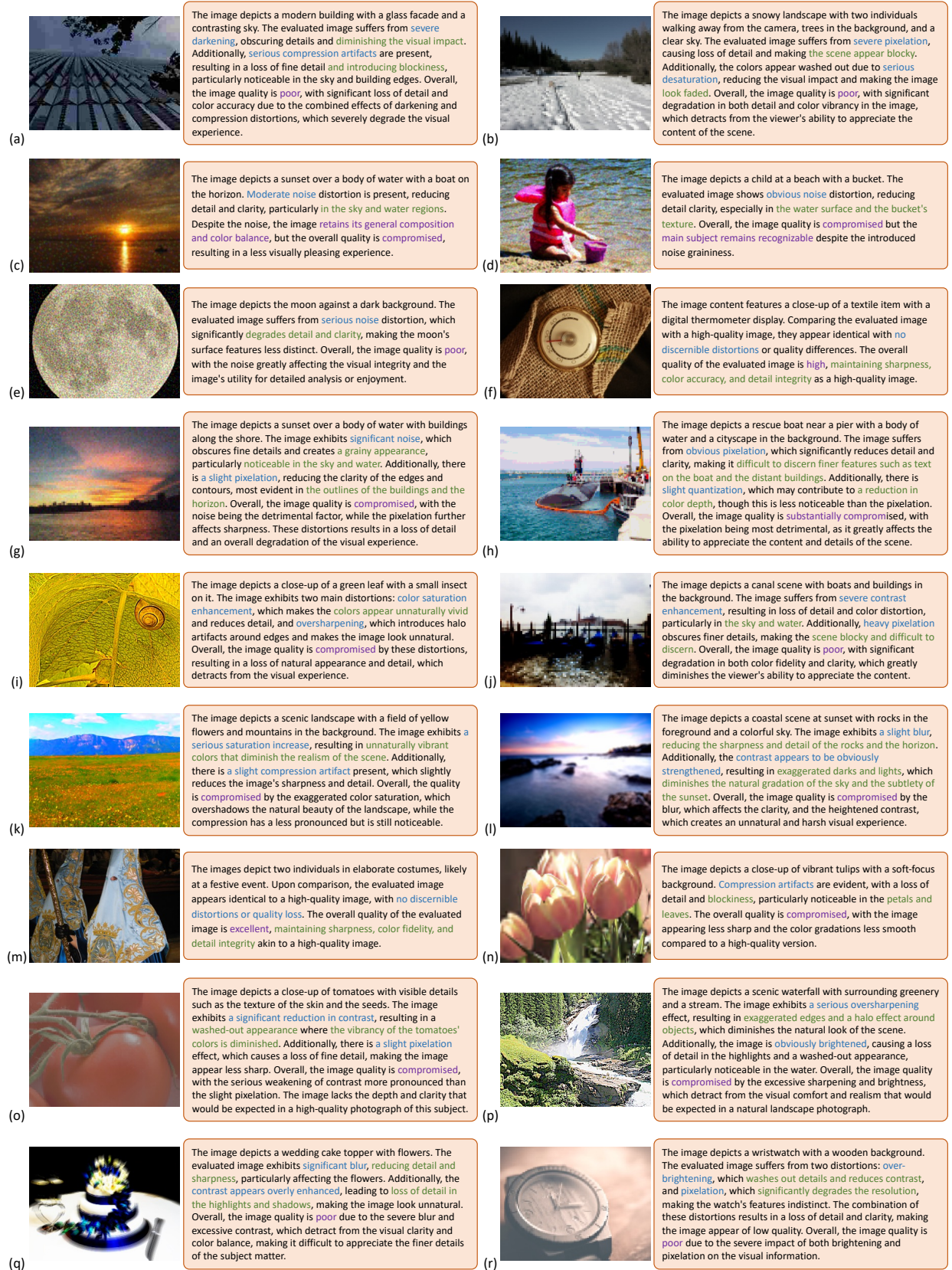


Fig. S5: Qualitative results on assessment reasoning task in the non-reference setting.

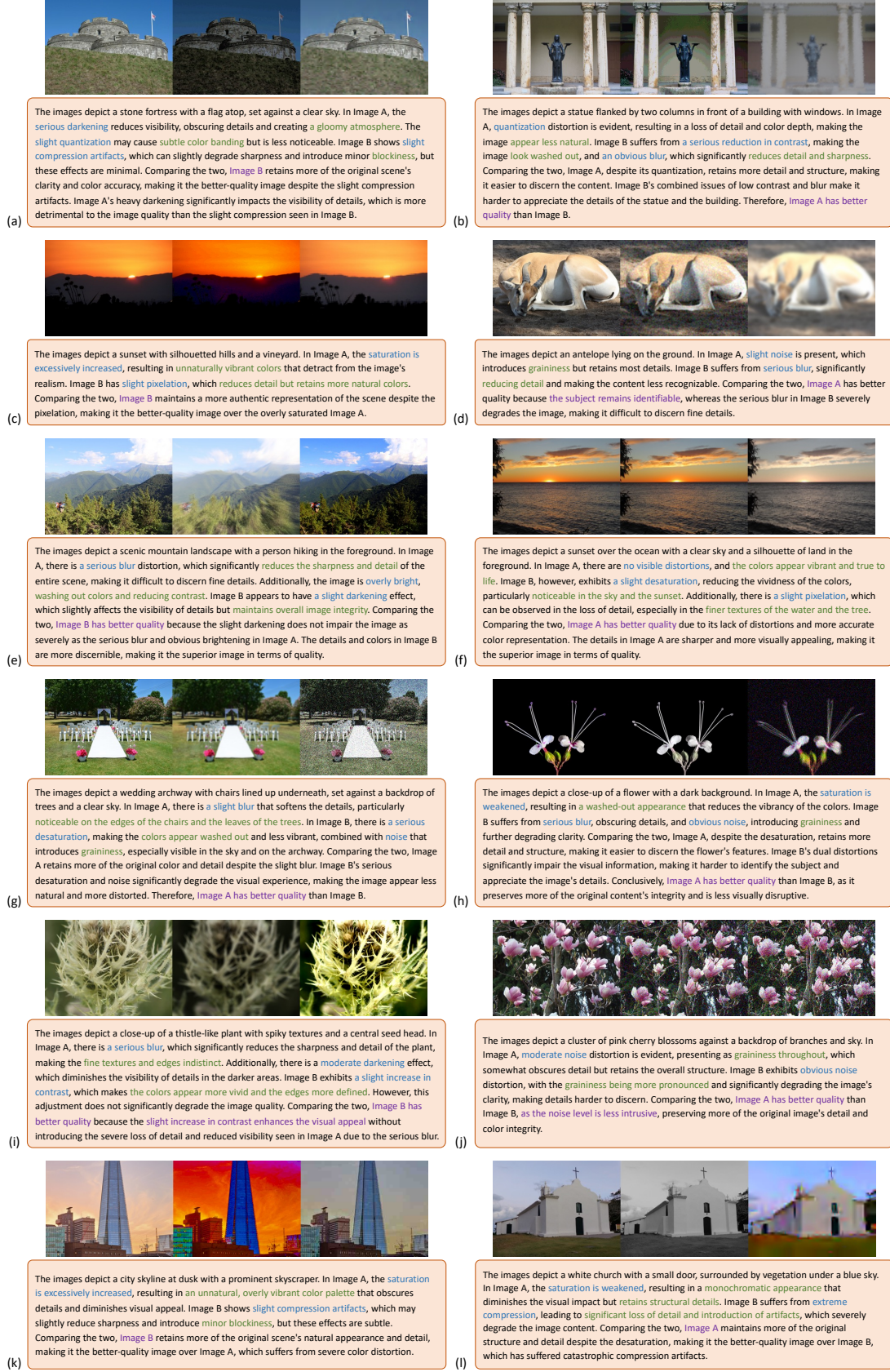


Fig. S6: **Qualitative results** on *comparison reasoning* task in the full-reference setting. The three images from left to right are the reference image, Image A, and Image B, respectively.



Fig. S7: **Qualitative results** on *comparison reasoning* task in the non-reference setting. The two images from top to down are Image A and Image B, respectively.



Fig. S8: Qualitative results on assessing web-downloaded images.